

bonding toward OH acids, and this is probably true also for NH and CH acids.

Acknowledgment. We are grateful to Profs. C. Laurence and M. Berthelot for providing us with their results prior to publication.

We extend our thanks for Prof. M. Chastrette for making available his PCA program ANALFACT and to Prof. R. W. Taft for helpful discussions.

Registry No. H⁺, 12408-02-5; K⁺, 24203-36-9.

Conformational Analysis of *N*-(1-Phenylethyl)- Δ^4 -thiazoline-2-thiones and Analogues. A ¹H NMR, Circular Dichroism, X-ray Crystallographic, and Molecular Mechanics Study

Jan Roschester,^{1a} Ulf Berg,^{1a} Marcel Pierrot,^{1b} and Jan Sandström*^{1a}

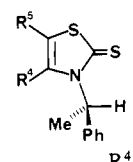
Contribution from the Division of Organic Chemistry 3, Chemical Center, University of Lund, S-221 00 Lund, Sweden, and Service de Cristallogimie, Centre Universitaire St. Jérôme, F-13013 Marseille, France. Received March 20, 1986

Abstract: The conformations of eleven *N*-(1-phenylethyl)thiazoline-2-thiones and three *N*-(1,2,3,4-tetrahydro-1-naphthyl) analogues with a variety of substituents in positions 4 and 5 have been studied by temperature-dependent ¹H NMR and CD spectra, by empirical force-field calculations and in two cases by single-crystal X-ray diffraction. The expected syn-anti equilibrium with respect to the N-substituent is much more biased toward the anti form than in the *N*-isopropyl and *N*-(1-carbomethoxyethyl) analogues. Only the compounds with a 4-phenyl substituent display observable populations of the syn form, and the X-ray diffraction studies show the 4-methyl and 4-phenyl-5-methyl compounds to adopt the anti form in the crystal. Five CD bands in the near UV region are assigned to one $n \rightarrow \pi^*$ and two $\pi \rightarrow \pi^*$ transitions in the thiazolinethione chromophore and to the ¹L_b and ¹L_a transitions in the benzene ring. The temperature dependence of the two thiazoline-thione bands at longest wavelengths for the 4-H compounds is interpreted in terms of an equilibrium between two rotamers within the anti form, by using semiempirical calculations of rotational strengths and experimental temperature-dependent ¹H chemical shifts. Corresponding energy minima are found by the molecular mechanics calculations.

A molecular system, composed of a rigid planar framework with an attached sp³-hybridized atom carrying three different substituents, a chiral rotor, displays a circular dichroism (CD) spectrum, the appearance of which depends on the orientation of the rotor. The signs and magnitudes of the rotational strengths of the electronic transitions in the molecule can in principle be calculated by semiclassical² or quantum-chemical³ methods, if the geometry of the molecule is known. Thus the CD spectrum contains stereochemical information, and this work is a part in a series planned to investigate the possibilities to elucidate the orientation of chiral rotors with respect to planar frameworks by a combined analysis of temperature-dependent CD and NMR spectra.

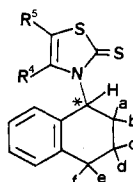
We have chosen the thiazoline-2-thione system as the planar framework for the following reasons: 1. Its electronic transitions have been studied both experimentally and by CNDO/S^{4,5} and PPP^{5,6} calculations. 2. The conformations of its *N*-isopropyl and *N*-(1-carboxyethyl) derivatives have been studied by ¹H NMR technique.^{7,8} 3. It gives rise to a $n \rightarrow \pi^*$ and several $\pi \rightarrow \pi^*$

Chart I



R ⁵	R ⁴				
	H	Me	Et	<i>i</i> -Pr	Ph
H	1	2		3	4
Me	5	6	7	8	9
Ph	10	11			

Chart II



R ⁵	R ⁴		
	H	Me	Ph
H	12	13	
Me			14

transitions, and since the rotational strengths of these two kinds of transitions follow different geometric rules,² complementary conformational information can be expected.

We have chosen a 1-phenylethyl group attached to the nitrogen atom as the chiral rotor, because the transition energies and

(1) (a) Chemical Center, Lund. (b) Centre Universitaire St. Jérôme, Marseille.

(2) Schellman, J. A. *Acc. Chem. Res.* **1968**, *1*, 144-151.

(3) Hansen, A. E.; Bouman, T. D. *Adv. Chem. Phys.* **1980**, *44*, 545-644.

(4) Pfister-Guillouzo, G.; Gonbeau, D.; Deschamps, J. J. *Mol. Struct.* **1972**, *14*, 95-111.

(5) Bouin, I.; Roussel, C.; Chanon, M.; Metzger, J. J. *Mol. Struct.* **1974**, *22*, 389-400.

(6) Bouscasse, L.; Chanon, M.; Phan-Tan-Luu, R.; Vincent, J. E.; Metzger, J. *Bull. Soc. Chim. Fr.* **1972**, 1055-1062.

(7) Roussel, C.; Lidén, A.; Chanon, M.; Metzger, J.; Sandström, J. *J. Am. Chem. Soc.* **1976**, *98*, 2847-2852.

(8) Blaise, B.; Roussel, C.; Metzger, J.; Sandström, J. *Can. J. Chem.* **1980**, *58*, 2212-2220.

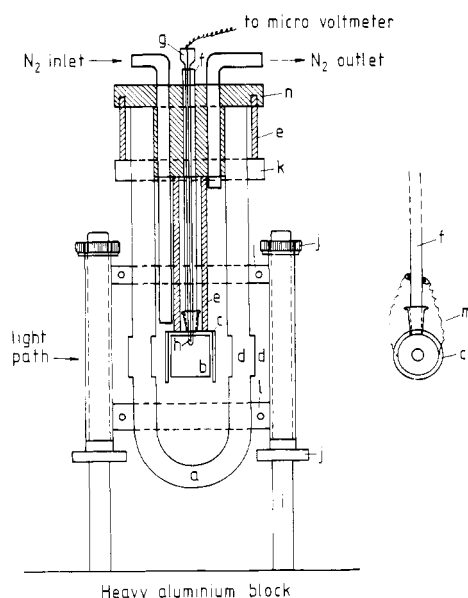


Figure 1. Vessel for variable-temperature CD measurements: (a) silvered Dewar vessel; (b) quartz cuvette; (c) cell holder; (d) quartz windows; (e) metal rod; (f) glass tube with ground joint to cuvette; (g) glass capillary for thermocouple; (h) copper-constantan thermocouple; (i) threaded brass rod; (j) interior screw; (k) Teflon ring; (l) steel band to hold Dewar; (m) steel wire spring to hold cuvette; (n) Teflon lid. The temperature is stable to $\pm 0.2^\circ\text{C}$.

directions of the transition moments in the benzene chromophore are well known. The 1-phenylethyl compounds are found in Chart I.

Similar systems with less torsional freedom for the benzene ring are found in *N*-(1,2,3,4-tetrahydro-1-naphthyl)thiazoline-2-thiones, and three members of this group have been included in the study (Chart II).

Unfortunately, attempts to prepare analogues with a *tert*-butyl group in position 4 have not been successful.

Experimental Section

^1H NMR spectra were recorded with a Nicolet Model 360 WB and/or a JEOL Model MH-100 NMR spectrometer. The samples for low-temperature studies were ca. 0.08 M in dimethyl ether- d_6 (360 MHz) or ca. 0.6 M in toluene- d_8 (100 MHz), and they were degassed by several cycles of freezing and thawing under high vacuum before being sealed off.

The first-order rate constants, k , for the observed exchange processes were evaluated from the exchange-broadened spectra by visual fitting of spectra, calculated by the McConnell expression for the bandshape of uncoupled two-site exchange systems^{10,11} to the experimental spectra. The temperature controller of the Nicolet instrument was calibrated by using the chemical shift difference in a methanol sample in dimethyl ether- d_6 , which in turn had been calibrated with the JEOL MH-100 instrument, by using the technique previously described.⁹ The T_2 values were obtained from the bandwidth of the resonance of added dimethyl oxalate.¹² The free energies of activation, ΔG^\ddagger , were calculated by using the Eyring equation¹³ in the form $\Delta G^\ddagger = RT \ln(k_B T/hk)$.

CD spectra were recorded on a JASCO Model J41-A spectrometer. The variable-temperature spectra were obtained with the measuring cell inside a silvered Dewar vessel with two interior and two exterior fused quartz windows (Figure 1). Cooling was accomplished by boiling off liquid nitrogen from an attached Dewar vessel, and the temperature was regulated with the boiling rate and monitored by a copper-constantan thermocouple dipping into the sample. The possibility of a temperature-dependent birefringence of the quartz windows was checked as proposed by Nordén¹⁴ and was found negligible. Correction for thermal contraction was made.¹⁵

Optical rotations were measured on Perkin Elmer Model 141 and 241 MC polarimeters and UV spectra on Cary Models 118 and 119 spectrophotometers. Mass spectra are from a Finnigan Model 4021 mass spectrometer and melting points (uncorrected) from a Leitz microscope heating stage Model 350.

Molecular mechanics (MM) calculations were performed by using the MM2 force field¹⁶ with the interactive computer graphics program MOLBUILD.¹⁷ Calculations were performed on 3-isopropyl-4-methylthiazoline-2-thione and on **1**, **2**, **12**, and **13**, in all cases with a rigid thiazoline ring. With systems **1**, **2**, and the 3-isopropyl analogue of **2**, the rotor was driven incrementally in steps of 10° , allowing complete relaxation of all geometric variables except the C4-N3-C31-C32 dihedral angle (see head of Table III for numbering). In this way, four energy minima were found on the rotation itinerary. With the geometries from the respective lowest energy minima, energy maps were calculated for **1** and **2** with grids from the C4-N3-C31-C1' angle (the rotor angle, ϕ_1) and N3-C31-C1'-C2' angle (the phenyl angle, ϕ_2), by using only the van der Waals terms (rigid rotation). These maps showed only the two lowest energy minima, the other two appearing as terraces in the slopes, but when the low-energy regions were recalculated by using the complete force field, the terraces changed to real minima. The energy maps are shown in Figure 2.

With **12** and **13**, the energy surface determined by ϕ_1 and a H-C2-C3-H dihedral angle in the tetrahydronaphthalene unit was explored. Four energy minima were found, corresponding to half-chair conformations of the cyclohexene ring, with the thiazolinethione group pseudoaxial in two and pseudoequatorial in two minima. The angles ϕ_1 and ϕ_2 and energies for all energy minima in **1**, **2**, **12**, and **13** are found in Table VI, and the nonstandard force-field parameters in Table I.

The CNDO/S calculations were performed with the program described by Pfister-Guillouzo et al.,¹⁸ which includes d orbitals in the basis set for sulfur. Excited states were generated by configuration interaction (CI) between the 99 lowest singly excited states. The monopoles of the transition charge density (vide infra) were obtained by $q_i = \sum_r C_r q_{ir}$, where C_i is the CI coefficient for excited state $0 \rightarrow i$, and q_{ir} is the transition monopole for this excitation. Since the CNDO/S calculations give good dipole moments for simple heterocyclic compounds, this program has also been used to calculate static charges. We have found this program to give charges, which differ only slightly from those obtained by the standard CNDO/2 program in compounds containing only first-row elements.

Theoretical CD spectra were calculated by using the matrix formalism developed by Schellman et al.¹⁹ The input consists of the magnitudes and directions of the electric transition moments of the $\pi \rightarrow \pi^*$ transitions and of the magnitudes and locations of the corresponding transition charge densities, of the strength and direction of the magnetic transition moment of the $n \rightarrow \pi^*$ transition of the thiazoline-2-thione, of the magnitudes and locations of the charges in the corresponding transition quadrupole, of the static charges of all atoms, and of the energies of all the transitions involved. The program allows the simultaneous use of three mechanisms for generation of rotational strength: (1) interactions of $\pi \rightarrow \pi^*$ transitions in different chromophores through dipole-dipole coupling (the coupled oscillator mechanism),²⁰ (2) interactions between $n \rightarrow \pi^*$ and $\pi \rightarrow \pi^*$ transitions in different chromophores through dipole-quadrupole couplings (the μ -m mechanism),²¹ and (3) "mixing" of $n \rightarrow \pi^*$ and $\pi \rightarrow \pi^*$ transitions in the same chromophore through perturbation by chirally disposed static charges (the one-electron mechanism).²²

The input is collected in Table XI. The signs of the transition charges (MP and QP) match the chosen directions of the transition dipoles (μ and M).

The magnitudes of the electric transition dipoles, μ (in D), are obtained from experimental spectra, by using the expression $\mu^2 = 9.18 \cdot 10^{-3} \int (\epsilon/\lambda) d\lambda = 9.18 \cdot 10^{-3} \epsilon_{\max} \Delta \sqrt{\pi/\lambda_{\max}}$, where Δ is half the width of the band when $\epsilon = \epsilon_{\max}/e$ (exponential halfwidth), assuming Gaussian

(9) Lidén, A.; Roussel, C.; Liljefors, T.; Chanon, M.; Carter, R. E.; Metzger, J.; Sandström, J. *J. Am. Chem. Soc.* **1976**, *98*, 2853-2860.

(10) McConnell, H. M. *J. Chem. Phys.* **1958**, *28*, 430-438.

(11) Rogers, M. T.; Woodbrey, J. C. *J. Phys. Chem.* **1962**, *66*, 540-546.

(12) Lidén, A.; Sandström, J. *Tetrahedron* **1971**, *27*, 2893-2901.

(13) Glasstone, S.; Laidler, K. J.; Eyring, H. *The Theory of Rate Processes*; McGraw-Hill: New York, 1941; p 195.

(14) Nordén, B. *Spectrochim. Acta* **1976**, *32A*, 441.

(15) (a) Korver, O.; Bosma, J. *Anal. Chem.* **1971**, *43*, 1119-1120 (EPA). (b) Passerini, R.; Ross, J. G. *J. Sci. Instr.* **1953**, *30*, 274-276 (methanol).

(16) Allinger, N. L.; Yuh, Y. H. *QCPE* **1980**, *11*, 395.

(17) Liljefors, T. *J. Mol. Graphics* **1983**, *1*, 111-117.

(18) Guimon, C.; Gonbeau, D.; Pfister-Guillouzo, G. *Tetrahedron* **1973**, *29*, 3399-3405.

(19) (a) Bayley, P. M.; Nielsen, E. B.; Schellman, J. A. *J. Phys. Chem.* **1969**, *73*, 228-243. (b) Rizzo, V.; Schellman, J. A. *Biopolymers* **1984**, *23*, 435-470.

(20) (a) Kirkwood, J. G. *J. Chem. Phys.* **1937**, *5*, 479-491. (b) Harada, N.; Nakanishi, K. *Circular Dichroic Spectroscopy—Exciton Coupling in Organic Stereochemistry*; Oxford University Press: 1983.

(21) Tinoco, I., Jr. *Adv. Chem. Phys.* **1962**, *4*, 113-160.

(22) Condon, E. U.; Altar, W.; Eyring, H. *J. Chem. Phys.* **1937**, *5*, 753-775.

Table I. Nonstandard Force-Field Parameters (Energies in kcal/mol)^a

Stretching Parameters			
$E_s = 71.94k_s(l - l_0)^2[1 + C_s(l - l_0)]$; $C_s = -2.00$			
bond type	k_s (mdyn Å ⁻¹)	l_0 (Å)	
C(sp ² , carbonyl)-S(thione)	5.14	1.670	
C(sp ²)-C(sp ²)	9.6	1.3923	
Bending Parameters			
$E_B = 0.021914k_B(\theta - \theta_0)^2[1 + C_f(\theta - \theta_0)^4]$			
angle type	θ_0 (degree)	k_B (mdyn Å rad ⁻²)	
C(sp ²)-C(sp ³)-N(sp ²)	109.47	0.42	
H-C(sp ³)-N(sp ²)	109.47	0.42	
C(sp ³)-C(sp ³)-N(sp ²)	109.47	0.42	
C(sp ³)-N(sp ²)-C(sp ²)	112.7	0.4	
C(sp ³)-N(sp ²)-C(sp ² , carbonyl)	112.7	0.4	
H-C(sp ²)-N(sp ²)	110.0	0.4	
H-C(sp ²)-S(in the ring)	126.0	0	
C(sp ² , carbonyl)-S(thione) ^b	0.0	0.8	
N(sp ²)-C(sp ² , carbonyl)-S(thione)	125.0	0.5	
S(thione)-C(sp ² , carbonyl)-S(in the ring)	125.6	0.5	
C(sp ³)-C(sp ²)-N(sp ²)	124.1	0.5	
Torsional Parameters			
$E_t = 1/2[V_1(1 + \cos(w)) + V_2(1 - \cos(2w)) + V_3(1 + \cos(3w))]$			
angle type	V_1 (kcal mol ⁻¹)	V_2 (kcal mol ⁻¹)	V_3 (kcal mol ⁻¹)
C(sp ²)-C(sp ²)-C(sp ³)-N(sp ²)	0	0	0.6
C(sp ²)-C(sp ³)-N(sp ²)-C(sp ²)	0	0	0.24
C(sp ²)-C(sp ³)-N(sp ²)-C(sp ² , carbonyl)	0	0	0.24
C(sp ³)-N(sp ²)-C(sp ²)-C(sp ²)	0	1.2	0
C(sp ³)-N(sp ²)-C(sp ²)-H	0	1.43	0
C(sp ³)-N(sp ²)-C(sp ² , carbonyl)-S(in the ring)	0	6.0	0
C(sp ³)-N(sp ²)-C(sp ² , carbonyl)-S(thione)	0	6.0	0
C(sp ³)-C(sp ³)-C(sp ³)-N(sp ²)	0	0	0.50
H-C(sp ³)-C(sp ³)-N(sp ²)	0	0	0.50
C(sp ²)-N(sp ²)-C(sp ³)-H	0	0	0.24
C(sp ² , carbonyl)-N(sp ²)-C(sp ³)-H	0	0	0.24
C(sp ³)-C(sp ³)-N(sp ²)-C(sp ²)	0	0	0.24
C(sp ³)-C(sp ³)-N(sp ²)-C(sp ² , carbonyl)	0	0	0.24
H-C(sp ²)-C(sp ²)-S(in the ring)	0	15.0	-1.06
C(sp ² , carbonyl)-N(sp ²)-C(sp ²)-H	0	1.43	0
C(sp ² , carbonyl)-S(in the ring)-C(sp ²)-H	0	0	0
H-C(sp ²)-C(sp ²)-N(sp ²)	0	0	0
C(sp ²)-N(sp ²)-C(sp ² , carbonyl)-S(thione)	0	6.0	0
C(sp ²)-S(in the ring)-C(sp ² , carbonyl)-S(thione)	0	6.0	0
C(sp ³)-N(sp ²)-C(sp ²)-C(sp ³)	-0.1	1.43	0
H-C(sp ³)-C(sp ²)-N(sp ²)	0	0	0
C(sp ³)-C(sp ²)-C(sp ²)-S(in the ring)	-0.1	15.0	-1.06
C(sp ³)-C(sp ²)-N(sp ²)-C(sp ² , carbonyl)	-0.1	1.43	0
C(sp ³)-C(sp ²)-C(sp ²)-H	-0.93	9.0	0
C(sp ²)-C(sp ²)-C(sp ²)-C(sp ²)	-0.93	9.0	0
H-C(sp ²)-C(sp ²)-H	-0.93	9.0	0
C(sp ³)-C(sp ²)-C(sp ²)-C(sp ²)	-0.93	9.0	0
C(sp ³)-C(sp ²)-C(sp ²)-H	-0.93	9.0	0

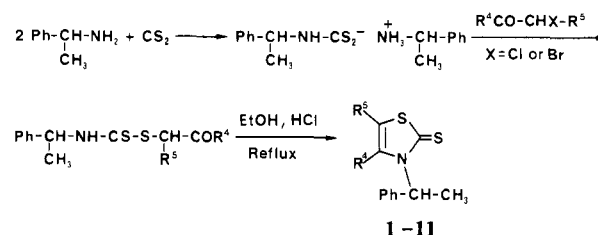
^a The motion of the atoms in the thiazoline ring has been restricted in all directions during minimization. ^b Out-of-plane bending.

bandshape. The data for the benzene chromophore are calculated from toluene spectra, and the band in vacuum UV is taken from the work of Shorygin et al.²³ The tetrahydronaphthalene unit was initially (vide infra) treated as an *o*-xylene chromophore, and the data were taken from the work of Jones and Taylor.²⁴ The direction of the transition moment of the first $\pi \rightarrow \pi^*$ transition in the thiazolinethione chromophore is taken from a CNDO/S calculation. The value for the angle α (8.8°, Table XI) agrees well with the 10.6° found by Bouman and Hansen²⁵ in a RPA calculation with a 4-31G basis. The transition charge densities are taken from CNDO/S calculations and scaled to agree with the experimental transition moments. The individual charges are distributed

Table II. Crystal Data and Refinement Parameters for **2** and **9**

	2	9
formula	C ₁₂ H ₁₃ NS ₂	C ₁₈ H ₁₇ NS ₂
formula wt	235.37	311.47
space group	monoclinic, $P2_1/c$	orthorhombic, $P2_12_12_1$
<i>a</i> , Å	7.821 (4)	12.327 (6)
<i>b</i> , Å	10.606 (5)	12.326 (6)
<i>c</i> , Å	14.587 (7)	10.529 (5)
β , deg	99.30 (9)	90
<i>V</i> , Å ³	1194	1599
<i>Z</i>	4	4
<i>d</i> _{calcd} g/cm ³	1.31	1.29
μ cm ⁻¹	3.9	3.1
no. of obsrvtns	1674	1242
(<i>I</i> > 3 σ (<i>I</i>))		
no. of variables	136	190
<i>R</i> ^a	0.046	0.031
<i>R</i> _w ^b	0.045	0.033
esd of an obsrvtn of unit wt	0.779	0.738
(shift/error) _{max}	0.21	0.32

^a $R = \sum ||F_o| - |F_c|| / \sum |F_o|$. ^b $R_w = [\sum w(|F_o| - |F_c|)^2 / \sum w|F_o|^2]^{1/2}$, $w = 1/\sigma^2(|F_o|)$.

Scheme I

as monopoles (MP) in the centre of gravity of the *p* orbital lobes at distances *R* above and below the individual nuclei, with $R = Ka_0/LA$,^{26a} where *K* is 15 for first-row and 63 for second-row elements,^{26b} *a*₀ is the Bohr radius (0.529 Å), *L* is 4 for first-row and 8 for second-row elements, and *Z* is the effective nuclear charge.

The magnetic transition moment for the $n \rightarrow \pi^*$ transition, *M*, is calculated by eq 1,²⁷

$$M = \sqrt{2} \sum_i C_i C_i^* \langle \psi(3p_z, S) | (e/2mc) \cdot \mathbf{r} \times \mathbf{p} | \psi(3p_z, S) \rangle = i\beta i \sqrt{2} \sum_i C_i C_i^* \quad (1)$$

where *r* and *p* are the position and linear momentum operators, *C_i* is the coefficient for $\psi(3p_z, S)$ in the $0 \rightarrow i$ excitation contributing to the $n \rightarrow \pi^*$ excited state, β is a Bohr magneton ($9.273 \cdot 10^{-21}$ erg/G), and *i* is the unit vector along the C=S bond. The charges in the transition quadrupole for the $n \rightarrow \pi^*$ transition, QP, are located in the *yz* planes at C2 and S2 (the *x* axis along C2-S2) and are calculated by eq 2,

$$QP = \sqrt{2} \sum_i C_i C_i^* \langle \psi(n) | \psi(\pi^*) \rangle = \left(e \sqrt{2} / \pi \right) \sum_i C_i C_i^* \quad (2)$$

where *C_i* and *C_i*^{*} are the appropriate LCAO coefficients for C2 and S2, respectively. The integration in eq 2 is performed between the positive *y* and *z* axes. The coordinates for QP are calculated by $y, z = \pm K\pi a_0 / 16Z$.²⁶

By using bond lengths and angles from the lowest energy minimum of **1** and a grid of ϕ_1 (0 to 360°) and ϕ_2 (0 to 180°) with intervals of 10°, maps of rotational strengths for all transitions under consideration have been calculated. By superposition of these maps with those from the energy calculations, the theoretical rotational strengths in the regions around the energy minima are readily found.

X-ray Crystallographic Data. Crystals of (*R,S*)-**2** and (*S*)-**9** were mounted on a CAD-4 Enraf-Nonius diffractometer equipped with a graphite monochromator for Mo K α radiation (0.71073 Å). Unit cell parameters were refined by least-squares treatment of $\sin \theta / \lambda$ values for 25 reflections ($15^\circ < \theta < 20^\circ$). Intensities were measured by using an ω -2 θ scan technique. Periodically monitored check reflections displayed

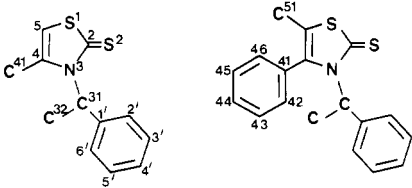
(23) Shorygin, P. P.; Petrukhov, V. A.; Khomenko, A. Kh.; Chernyshev, E. A. *Russ. J. Phys. Chem.* **1968**, *42*, 555-559.

(24) Jones, L. C., Jr.; Taylor, L. W. *Anal. Chem.* **1955**, *27*, 228-237.

(25) Bouman, T. D.; Hansen, A. E., personal communication.

(26) (a) Woody, R. W. *J. Chem. Phys.* **1968**, *49*, 4797-4806. (b) Derived as in ref 26a for second-row elements, by using Slater orbitals.

(27) Woody, R. W.; Tinoco, I., Jr. *J. Chem. Phys.* **1967**, *46*, 4927-4945.

Table III. Positional Parameters for Non-Hydrogen Atoms in **2** and **9**


atom	2			9		
	x^a	y	z	x	y	z
S1	0.5430 (1)	0.2026 (1)	0.25391 (8)	0.23011 (9)	0.1258 (1)	0.4585 (1)
C2	0.6938 (4)	0.2281 (3)	0.1813 (2)	0.2123 (3)	0.1320 (3)	0.2963 (4)
N3	0.7882 (3)	0.3317 (2)	0.2114 (2)	0.3004 (2)	0.1800 (3)	0.2426 (3)
C4	0.7419 (4)	0.3908 (3)	0.2900 (2)	0.3821 (3)	0.2097 (3)	0.3283 (4)
C5	0.6100 (5)	0.3330 (4)	0.3201 (3)	0.3582 (3)	0.1856 (3)	0.4494 (4)
S2	0.7074 (1)	0.13592 (9)	0.09085 (7)	0.1006 (1)	0.0849 (1)	0.2259 (1)
C31	0.9218 (4)	0.3792 (3)	0.1587 (2)	0.3067 (3)	0.1932 (4)	0.1018 (4)
C32	1.1029 (4)	0.3684 (4)	0.2155 (3)	0.4066 (4)	0.1381 (4)	0.0467 (4)
C1'	0.8722 (4)	0.5073 (3)	0.1170 (2)	0.2894 (3)	0.3115 (4)	0.0644 (4)
C2'	0.9964 (5)	0.5939 (4)	0.1006 (2)	0.3580 (4)	0.3636 (4)	-0.0199 (5)
C3'	0.9472 (6)	0.7070 (4)	0.0572 (3)	0.3374 (4)	0.4692 (4)	-0.0567 (5)
C4'	0.7759 (7)	0.7353 (4)	0.0301 (3)	0.2476 (5)	0.5222 (4)	-0.0131 (6)
C5'	0.6533 (6)	0.6512 (4)	0.0455 (3)	0.1776 (4)	0.4711 (4)	0.0711 (6)
C6'	0.6993 (5)	0.5375 (3)	0.0880 (3)	0.1987 (4)	0.3650 (4)	0.1081 (5)
C41	0.8339 (5)	0.5030 (4)	0.3336 (3)	0.4856 (3)	0.2588 (3)	0.2878 (4)
C42				0.4913 (4)	0.3656 (3)	0.2493 (5)
C43				0.5887 (4)	0.4085 (4)	0.2092 (5)
C44				0.6805 (4)	0.3460 (4)	0.2084 (4)
C45				0.6762 (3)	0.2388 (4)	0.2501 (5)
C46				0.5789 (3)	0.1965 (4)	0.2889 (4)
C51				0.4256 (4)	0.2037 (4)	0.5664 (4)

^aesd's in the least significant figure are given in parentheses in this and subsequent tables.Table IV. Bond Distances in **2** and **9** (in Å)

bond	2	9
S1-C2	1.729 (4)	1.723 (5)
S1-C5	1.719 (4)	1.746 (5)
C2-N3	1.356 (4)	1.360 (6)
C2-S2	1.660 (4)	1.667 (5)
N3-C4	1.404 (4)	1.401 (6)
N3-C31	1.482 (4)	1.494 (6)
C4-C41	1.479 (5)	1.476 (6)
C4-C5	1.334 (5)	1.342 (7)
C5-C51		1.502 (7)
C31-C32	1.525 (5)	1.522 (7)
C31-C1'	1.514 (5)	1.525 (5)
C1'-C2'	1.386 (5)	1.385 (7)
C1'-C6'	1.387 (5)	1.377 (7)
C2'-C3'	1.382 (7)	1.381 (8)
C3'-C4'	1.368 (7)	1.365 (9)
C4'-C5'	1.355 (7)	1.388 (9)
C5'-C6'	1.376 (5)	1.390 (8)
C41-C42		1.378 (8)
C41-C46		1.383 (6)
C42-C43		1.379 (8)
C43-C44		1.369 (8)
C44-C45		1.304 (8)
C45-C46		1.370 (8)

Table V. Bond Angles in **2** and **9** (deg)

angle	2	9
S1-C2-S2	122.2 (2)	122.0 (3)
S1-C2-N3	108.5 (3)	109.2 (3)
S1-C5-C4	111.5 (3)	110.1 (4)
S1-C5-C51		121.2 (4)
S2-C2-N3	129.3 (3)	128.8 (4)
C2-S1-C5	92.4 (2)	92.4 (2)
C2-N3-C4	115.3 (3)	114.8 (4)
N3-C4-C5	112.3 (3)	113.4 (4)
N3-C4-C41	122.6 (3)	122.9 (4)
N3-C31-C32	111.3 (3)	111.8 (4)
N3-C31-C1'	110.9 (3)	110.7 (4)
C4-N3-C31	124.6 (3)	125.0 (4)
C4C5-C51		128.7 (5)
C5-C4-C41	125.1 (4)	123.7 (5)
C32-C31-C1'	116.2 (3)	116.2 (4)
C31-C1'-C2'	121.5 (4)	121.6 (5)
C31-C1'-C6'	120.3 (3)	119.0 (5)
C1'-C2'-C3'	120.2 (5)	120.3 (6)
C1'-C6'-C5'	120.7 (4)	120.6 (6)
C2'-C1'-C6'	118.1 (4)	119.2 (5)
C2'-C3'-C4'	120.7 (5)	120.4 (6)
C3'-C4'-C5'	119.6 (5)	120.1 (5)
C4'-C5'-C6'	120.7 (5)	119.3 (6)
C4-C41-C42		121.4 (4)
C4-C41-C46		119.3 (4)
C41-C42-C43		120.0 (5)
C41-C46-C45		121.0 (5)
C42-C43-C44		120.4 (5)
C42-C41-C46		119.4 (5)
C43-C44-C45		120.0 (5)
C44-C45-C46		119.2 (5)

no significant variations in intensity throughout the experiments. Crystal data and refinement parameters are given in Table II. All computations were performed on a PDP 11/44 computer (SDP software).²⁸ The structures were solved by direct methods²⁹ and completed by difference Fourier methods. Hydrogen atoms were located on Fourier maps but not refined. Full matrix least-squares refinement included anisotropic thermal parameters for all non-hydrogen atoms. Final difference Fourier synthesis did not reveal any peak of density $>0.3 \text{ e}\text{\AA}^{-3}$. Positional parameters for **2** and **9** are found in Table III, bond distances and angles in Tables IV and V, and perspective views in Figure 3.

(28) Frenz, B. A. In *Computing in Crystallography*; Schenck, H., Olthof-Hazekamp, R., van Koningsveld, H., Bassi, G., Eds.; Delft University Press: 1978; pp 64-77.

(29) Germain, G.; Main, P.; Woolfson, M. M. *Acta Crystallogr., Sect. A: Cryst. Phys., Diffraction, Theor. Gen. Crystallogr.* **1971**, *27A*, 368-376.

Materials. Compounds **1-11** were prepared according to the reaction sequence in Scheme I. The synthesis of **12-14** was performed analogously, starting from (R,S)-1-amino-1,2,3,4-tetrahydronaphthalene.

(R)-N-(1-Phenylethyl)ammonium (R)-N-(1-Phenylethyl)dithiocarbamate. (R)-1-Phenylethylamine (0.6 mol) was added dropwise with stirring at +5 °C to a solution of CS₂ (0.3 mol) in isopropyl acetate (250 mL). A colorless precipitate (89.5 g, 94% yield) formed spontaneously: mp 100 °C (dec); $[\alpha]_D^{25} +28.4^\circ$ (c 1.0, EtOH); ¹H NMR (100 MHz,

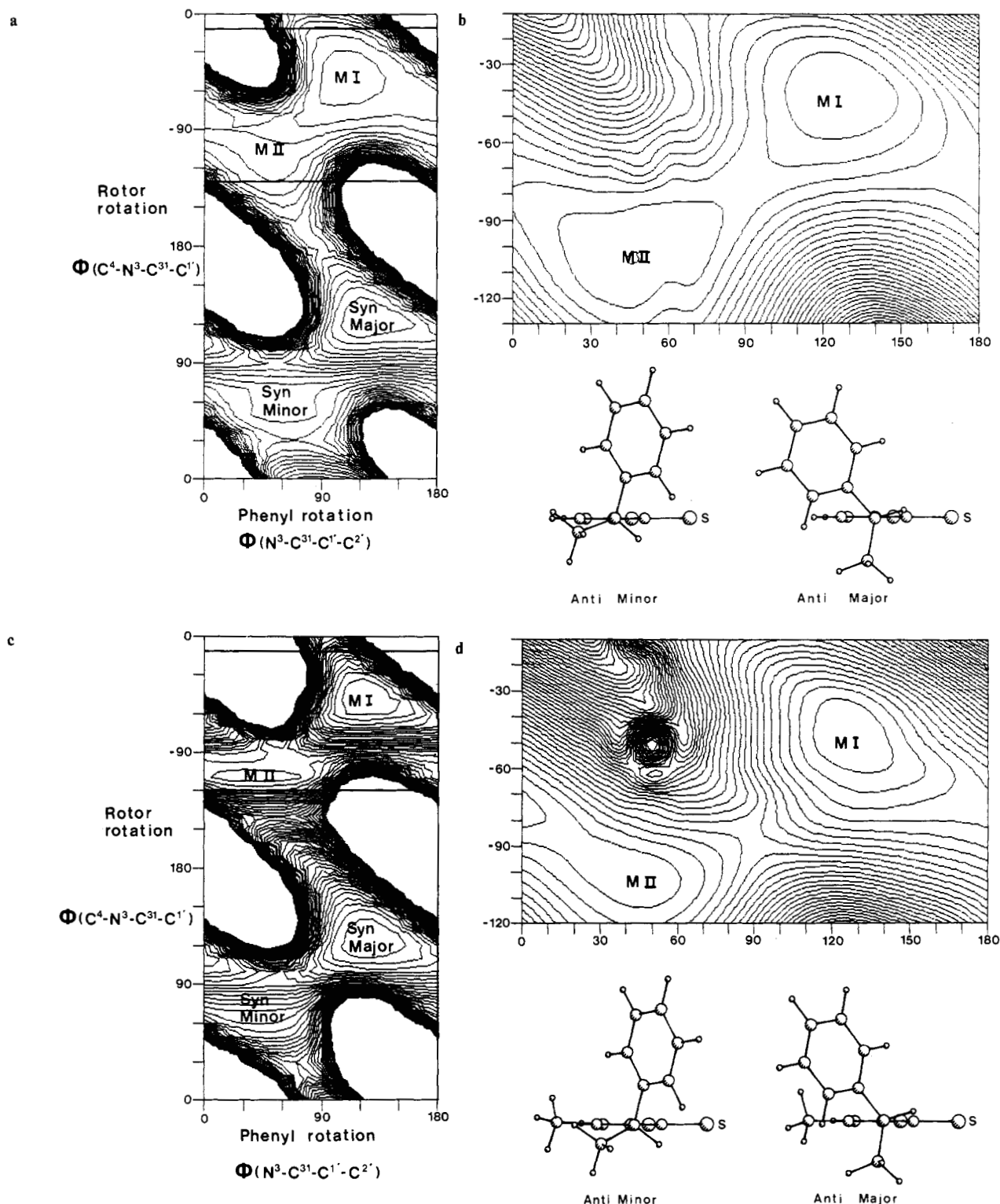


Figure 2. (a) van der Waals energy map for **1**; (b) minimized energy map of the anti region of **1**; (c) van der Waals energy map for **2**; (d) minimized energy map of the anti region of **2**. Energy equidistance for (a) and (c) 2.0 kcal/mol, for (b) and (d) 0.5 kcal/mol.

$\text{Me}_2\text{SO}-d_6$) 1.38 (3 H, d, $J = 7.0$ Hz, dithiocarbamate ion); 1.54 (3 H, d, $J = 6.8$ Hz, ammonium ion); 4.49 (1 H, q, $J = 7.0$ Hz); 5.71 (1 H, double q, br); 7.27 and 7.40 (10 H, m, Ar), 8.55 (1 H, d, $J = 8.7$ Hz, NH).

Triethylammonium (*R,S*)-*N*-(1,2,3,4-tetrahydro-1-naphthyl)dithiocarbamate was obtained as above as colorless prisms, in nearly quantitative yield from (*R,S*)-1-amino-1,2,3,4-tetrahydronaphthalene, CS_2 , and triethylamine in diethyl ether: ^1H NMR ($\text{Me}_2\text{SO}-d_6$) δ 1.08 (9 H, t, Et_3NH); 1.82 (4 H, br); 2.70 (2 H, br); 3.15 (7 H, q, overlapping multiplet Et_3NH and CH); 5.70 (1 H, br, NH in Et_3NH); 7.07 (4 H, m, Ar); 8.23 (1 H, d, br, $J = \text{ca. } 9$ Hz, NH in dithio-carbamate ion).

General Procedure for the Thiazoline-2-thiones 1–14. The appropriate halocarbonyl compound, dissolved in ethanol, was added dropwise with

stirring at $+5^\circ\text{C}$ to a solution of an equimolecular quantity of the appropriate dithiocarbamate in ethanol (in some cases DMF). The solution was kept overnight at room temperature, the solvent was evaporated, and the residue was dissolved in water and diethyl ether. The ether phase was dried and evaporated, and the residue was refluxed in 0.01 N HCl in ethanol until test samples showed constant UV absorption at 316 nm (<15 min for **1** to 24 h for **8**). Only **11** was formed in a spontaneous cyclization without heating or addition of acid. After evaporation, purification was effected by flash chromatography³⁰ on silica (Merck 60, 230–400 mesh) followed by recrystallization. The yields are

(30) Still, W. C.; Kahn, M.; Mitra, A. *J. Org. Chem.* **1978**, *43*, 2923–2925.

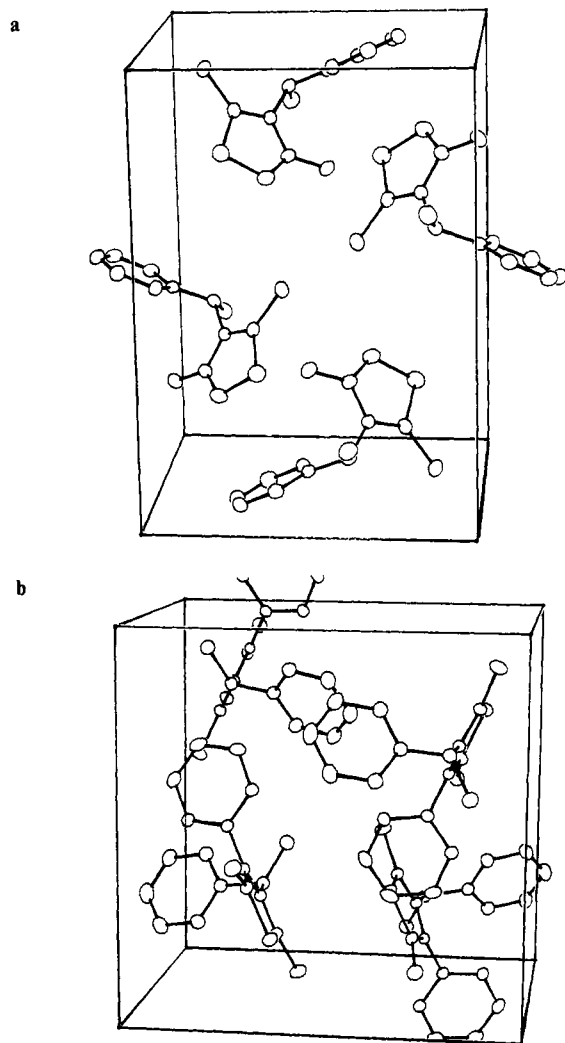


Figure 3. (a) Unit cell of 2; (b) unit cell of 9.

given for pure products. NMR spectra are given in Table VIII.

(R)-3-(1-Phenylethyl)- Δ^4 -1,3-thiazoline-2-thione (1): 38% yield; noncrystalline; $[\alpha]_D^{25} +377^\circ$ (*c* 0.93, EtOH); MS [IP 70 eV; *m/e* (% rel intensity)]: 221 (8, M), 117 (19, M - PhCH=CH₂), 105 (100, PhCHCH₃). Anal. Calcd for (C₁₁H₁₁NS₂) C, H, N, S 29.0, found 29.5.

(R)-3-(1-Phenylethyl)-4-methyl- Δ^4 -1,3-thiazoline-2-thione (2): 70% yield after recrystallization from methanol; mp 74.5–75.5 °C; $[\alpha]_D^{25} +315^\circ$ (*c* 0.92, EtOH); MS, 235 (8, M), 131 (28, M - PhCH=CH₂), 105 (100, PhCHCH₃). Anal. (C₁₂H₁₃NS₂) C, H, N, S.

(S)-3-(1-Phenylethyl)-4-isopropyl- Δ^4 -1,3-thiazoline-2-thione (3): 63% yield after recrystallization from absolute ethanol; mp 114.5–115.5 °C; $[\alpha]_D^{25} -248^\circ$ (*c* 0.48, EtOH); MS, 263 (8, M), 159 (21, M - PhCH=CH₂), 105 (100, PhCHCH₃). Anal. (C₁₄H₁₇NS₂) C, H, N, S.

(S)-3-(1-Phenylethyl)-4-phenyl- Δ^4 -1,3-thiazoline-2-thione (4): 63% yield after recrystallization from absolute ethanol–toluene, mp 135–136.5 °C; $[\alpha]_D^{25} -214^\circ$ (*c* 0.50, EtOH); MS, 297 (5, M), 193 (26, M - PhCH=CH₂), 105 (100, Ph-CH-CH₃). Anal. (C₁₇H₁₅NS₂) C, H, N, S.

(S)-3-(1-Phenylethyl)-5-methyl- Δ^4 -1,3-thiazoline-2-thione (5): 69% yield; noncrystalline; $[\alpha]_D^{25} -331^\circ$ (*c* 0.49, EtOH); MS, 235 (8, M), 131 (33, M - PhCH=CH₂), 105 (100, PhCHCH₃). Anal. (C₁₂H₁₃NS₂) C, H, N, S calcd 27.2, found 26.7.

(S)-3-(1-Phenylethyl)-4,5-dimethyl- Δ^4 -1,3-thiazoline-2-thione (6): 86% yield, noncrystalline, $[\alpha]_D^{25} -261^\circ$ (*c* 0.58, EtOH); MS, 249 (11, M), 145 (52, M - PhCH=CH₂), 105 (100, Ph-CH-CH₃). Anal. (C₁₃-H₁₅NS₂) C, H, N, S.

(S)-3-(1-Phenylethyl)-4-ethyl-5-methyl- Δ^4 -1,3-thiazoline-2-thione (7): 66% yield; recrystallized from absolute ethanol; mp 130–131 °C, $[\alpha]_D^{25} -291^\circ$ (*c* 0.46, EtOH); MS, 263 (10 M), 159 (46, M - PhCH=CH₂), 105 (100, Ph-CH-CH₃). Anal. (C₁₄H₁₇NS₂) C, H, N, S.

(S)-3-(1-Phenylethyl)-4-isopropyl-5-methyl- Δ^4 -1,3-thiazoline-2-thione (8): 67% yield, recrystallized from absolute ethanol; mp 127.5–129 °C; $[\alpha]_D^{25} -215^\circ$ (*c* 0.50, EtOH); MS, 277 (5, M), 173 (41, M - PhCH=CH₂), 105 (100, PhCHCH₃). Anal. (C₁₅H₁₉NS₂) C, H, N, S.

(S)-3-(1-Phenylethyl)-4-phenyl-5-methyl- Δ^4 -1,3-thiazoline-2-thione (9): 38% yield, recrystallized from absolute ethanol; mp 135–149 °C (dec); $[\alpha]_D^{25} -174^\circ$ (*c* 0.46, EtOH); MS, 311 (5, M), 207 (40, M - PhCH=CH₂), 105 (100, PhCH-CH₃). Anal. (C₁₈H₁₇NS₂) C, H, N, S.

(S)-3-(1-Phenylethyl)-5-phenyl- Δ^4 -1,3-thiazoline-2-thione (10): low yield due to repeated chromatographic purifications, recrystallized from absolute ethanol; mp 108.5–109.5 °C, $[\alpha]_D^{25} -102^\circ$ (*c* 0.42, EtOH); MS, 297 (5, M), 193 (M - PhCH=CH₂); 105 (100; PhCHCH₃). Anal. (C₁₇H₁₅NS₂) C, H, N, S.

(S)-3-(1-Phenylethyl)-4-methyl-5-phenyl- Δ^4 -1,3-thiazoline-2-thione (11): 63% yield, recrystallized from absolute ethanol–toluene, mp 186–187 °C, $[\alpha]_D^{25} -178^\circ$ (*c* 0.459, CH₂Cl₂); MS, 311 (6, M), 207 (44, M - PhCH=CH₂), 105 (100, PhCHCH₃). Anal. (C₁₈H₁₇NS₂) C, H, N, S.

(R,S)-3-(1,2,3,4-Tetrahydro-1-naphthyl)- Δ^4 -1,3-thiazoline-2-thione (12): 55% yield after recrystallization from absolute ethanol; mp 87–88 °C; $[\alpha]_D^{25} +406^\circ$ (*c* 0.037, EtOH, *R* form); MS, 247 (9, M), 131 (100, C₁₀H₁₁). Anal. (C₁₃H₁₃NS₂) C, H, N, S.

(R,S)-3-(1,2,3,4-Tetrahydro-1-naphthyl)-4-methyl- Δ^4 -1,3-thiazoline-2-thione (13): 67% yield after recrystallization from absolute ethanol; mp 121–122 °C; $[\alpha]_D^{25} +248^\circ$ (*c* 0.060, EtOH, *R* form); MS, 261 (5, M), 131 (100, C₁₀H₁₁). Anal. (C₁₄H₁₅NS₂) C, H, N, S.

(R,S)-3-(1,2,3,4-Tetrahydro-1-naphthyl)-4-phenyl-5-methyl- Δ^4 -1,3-thiazoline-2-thione (14): 34% yield after recrystallization from absolute ethanol–toluene; mp 151–152 °C, $[\alpha]_D^{25} +293^\circ$ (*c* 0.080, EtOH, *R* form); MS, 337 (7, M), 131 (100, C₁₀H₁₁). Anal. (C₂₀H₁₉NS₂) C, H, N, S.

3-Isopropyl-4-phenyl-5-methyl- Δ^4 -1,3-thiazoline-2-thione was prepared analogously from isopropylammonium *N*-isopropylthiocarbamate in 43% yield after recrystallization from ethanol; mp 159–161 °C; MS, 249 (50, M), 207 (100, M - C₃H₇). Anal. (C₁₃H₁₅NS₂) C, H, N, S.

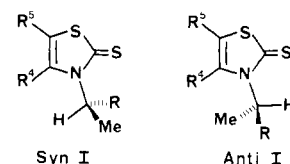
Starting Materials. Chloroethanol (for 1 and 12, 30% in H₂O), chloropropanone (for 2 and 13), 1-phenyl-2-bromoethanone (for 4), (*R*)-, (*S*)-, and (*R,S*)-1-phenylethylamine, and (*R,S*)-1-amino-1,2,3,4-tetrahydronaphthalene were all purchased from FLUKA AG and 3-chloro-2-butanone (for 6) from Merck-Schuchardt. 1-Bromo-3-methyl-2-butanone^{31,32} (for 3), 2-bromo-3-pentanone³¹ (for 7), 2-bromo-4-methyl-3-pentanone³¹ (for 8), 1-bromo-1-phenyl-2-propanone³² (for 11 and 14), 2-bromopropanal³² (for 5), 2-bromo-2-phenylethanal³³ (for 10), and 1-phenyl-2-bromo-1-propanone³³ (for 9) were all synthesized by published methods.

Compounds 12, 13, and 14 were obtained in enantiomerically pure form by preparative liquid chromatography on swollen microcrystalline triacetylcellulose.³⁴ Their absolute configurations were assigned based on the signs of CD bands 5 and 6 (vide infra), which are independent of the conformation for compounds 1–11.

No racemization occurred during the preparation of 1–11, as was established by the chiral shift reagent technique.³⁵ Surprisingly, no splitting of the ¹H resonances of the racemates occurred in any case by using Eu(hfbc)₃,³⁶ whereas either Eu(hfbc)₃ + Ag(fod)³⁷ or 2,2,2-trifluoro-1-(9-anthryl)ethanol (TFAE)^{35b} gave the desired results, except for 4, 10, and 11, but the optical purity of these compounds was assumed by analogy.

Results and Discussion

¹H NMR studies of 3-isopropyl- Δ^4 -thiazoline-2-thiones (I, R = CH₃)⁷ and their 3- α -carboxyethyl analogues (I, R = CO₂H or CO₂CH₃)⁸ have demonstrated the existence of two rotamers which can be designated syn I and anti I in conformity with the no-



menclature for pyrimidine nucleosides.³⁸ When R⁴ = H or *t*-Bu,

(31) Blaive, B. *Thèse de 3^{ème} cycle*; Université de Provence: Marseille, 1976.

(32) Roussel, C. *Thèse Sciences*; Université de Provence: Marseille, 1973.

(33) Bradsher, C. K.; Rosher, R. *J. Am. Chem. Soc.* **1939**, *61*, 1524–1525.

(34) Isaksson, R.; Roschester, J. *J. Org. Chem.* **1985**, *50*, 2519–2521.

(35) (a) Sullivan, G. R. *Top. Stereochem.* **1978**, *10*, 287–329. (b) Pirkle, W. H.; Hoover, D. J. *Top. Stereochem.* **1982**, *13*, 263–331.

(36) (a) Fraser, R. R.; Petit, M. A.; Saunders, J. K. *J. Chem. Soc., Chem. Commun.* **1971**, 1450–1451. (b) Goering, H. L.; Eikenberry, J. N.; Koerner, G. S. *J. Am. Chem. Soc.* **1971**, *93*, 5913–5914. (c) Whitesides, G. M.; Lewis, D. W. *J. Am. Chem. Soc.* **1971**, *93*, 5914–5915.

(37) Wenzel, T. J.; Sievers, R. E. *J. Am. Chem. Soc.* **1982**, *104*, 382–388.

Table VI. Energies (kcal/mol) and Dihedral Angles (deg) for Energy Minima (MM2) in **1**, **2**, **12**, and **13** and Dihedral Angles from Crystal Structures for **2** and **9**^a

compd	conformation		energy	rotor angle, ϕ_1 (C4-N3-C31-C1')	phenyl angle, ϕ_2 (N3-C31-C1'-C2')
1	syn		0.66	130.3	127.7
			2.96	70.5	53.1
1	anti	MI	0.00	-50.1	116.2
		MII	0.57	-103.5	49.7
2	syn		0.0	130.3	127.2
			2.51	72.9	43.7
2	anti	MI	0.27	-49.7	126.1
		MII	2.77	-101.5	37.1
2	crystal			-62.3	147.1
9	crystal			-76.0	127.1
12	syn		0.41 ^b	128.6	137.8
			2.45 ^c	149.4	113.8
12	anti	MIII ^b	0.00	-49.5	137.0
		MIV ^c	0.53	-33.4	109.8
13	syn		0.0 ^b	129.1	136.2
			2.37 ^c	147.9	115.7
13	anti	MIII ^b	0.14	-50.0	135.3
		MIV ^c	2.52	-32.9	112.7

^aR configuration. ^bThiazolinethione pseudoequatorial. ^cThiazolinethione pseudoaxial.

no exchange effects on the ¹H NMR spectra have been observed, due to a strong dominance of the anti and the syn rotamers, respectively. When R⁴ is intermediate in size, free energy barriers in the range 13.1–15.6 kcal/mol are observed between the syn and anti forms. The position of the equilibrium depends on the size of R⁴ and to lesser extent on that of R⁵, the syn form in general being favored by a large R⁴.

In the sequel, we will present experimental and theoretical results to demonstrate that compounds **1–14** appear in analogous forms, but that the equilibrium in general is much more in favor of the anti form. We will also demonstrate how temperature-dependent CD spectra can be used to elucidate finer conformational details not directly accessible by the NMR technique.

Molecular Mechanics (MM) Calculations. For the isopropyl analogue of **5** (I, R = R⁴ = CH₃, R⁵ = H), the syn form was found to have the lowest energy with the anti form as a double minimum at 0.7 kcal/mol higher energy. The syn → anti barrier was calculated to 10.0 kcal/mol. These results deviate from the experimental ones, since in acetone-*d*₆ solution the anti form is more stable by 0.53 kcal mol⁻¹, and the syn → anti barrier (ΔG^\ddagger) is 14.6 kcal/mol.⁷ The deviation for the ground-state energies is not alarming, since solvent effects may contribute. The deviation for the barrier is considerably larger than previously found for alkyl group rotations in amides and thioamides,^{9,39,40} but Jaime and Osawa⁴¹ have recently pointed out the tendency of the MM2 force field to underestimate high single bond barriers. They calculate the interring barrier in a 1-cyclohexylpiperidine to be 4 kcal mol⁻¹ below the expected one. In our case, the deviation between experimental and calculated energies for the isopropyl compound may be used for rough corrections of the calculated energies of compounds **1**, **2**, **12**, and **13**. For these, the deficiencies in the force field for aromatic rings⁴² introduce further uncertainty.

Incremental driving of the rotor in **1** gave a syn → anti barrier of 4.1 kcal/mol. Inspection of the energy map (Figure 2a) reveals two minima for the syn and two for the anti form (Table VI). The energy was calculated to be lowest for one of the anti minima, but the second anti and one syn minimum are quite close. The syn-anti barrier for **2** was calculated to 7.7 kcal/mol. Four energy minima were found, with one syn minimum lowest and one of the anti minima only slightly higher, but with the two other minima considerably higher in energy. The calculations for the tetra-

hydronaphthalene derivatives **12** and **13** also gave four energy minima, all with the tetrahydronaphthalene ring in half-chair form. Two are of the syn and two of the anti type, and in each pair the most stable form has a pseudoequatorial and the less stable a pseudoaxial thiazolinethione group (Figure 4). The anti form is calculated to be most stable for **12** and the syn form for **13**, and the two minima in the anti form of **12** are calculated to be quite close in energy. Due to the large number of geometric variables involved and the poor agreement for **2** (vide infra), we have not tried to calculate the rotational barriers for **12** and **13**.

As will be shown later, the anti form in **2** should be favored by at least 2.5 kcal/mol and by more in **1**, and the syn → anti barrier should be at least 12 kcal/mol in **2**. Thus the numerical agreement is not very satisfactory, i.e., the force field is probably far from adequate for these molecules. However, it is a general observation that the number and approximate location of energy minima is less sensitive to the force field than their energies, especially when no strong interactions are involved. This follows also from our work, since the positions of the minima found on the map created by a force field containing only nonbonding interactions do not differ much from those found by the full force field. Thus we propose the existence of two syn and two anti minima for all compounds **1–14**.

The calculated angles of rotation of the rotor (C4-N3-C31-C1', ϕ_1) and of the phenyl ring (N3-C31-C1'-C2', ϕ_2) in the energy minima, which are important for the theoretical calculations of the CD spectra, are found in Table VI together with data from the **X-ray crystallographic structures**. These show both **2** and **9** in anti form. For **2** the conformation is rather close to the calculated minimum energy structure although with a higher ϕ_2 value, possibly due to packing forces in the crystal. In **2** the methine C-H bond is only 2° and in **9** 10° out of the thiazoline plane. The C32H-S2 distances are 2.63 and 2.69 Å, respectively, shorter than the sum of the van der Waals radii, 3.5 Å,⁴³ but longer than the 2.51 and 2.37 Å found by Pèpe and Pierrot in two 3-isopropylthiazolinethiones.⁴⁴ In **9** the angle between the thiazolinethione and 4-phenyl planes is 74.5°, and in solution the phenyl ring can be expected to undergo libration around a nearly orthogonal conformation, in agreement with the ¹H NMR results to be discussed below.

¹H NMR Spectra. The spectra of all compounds were recorded at 360 MHz from ambient temperature to -130 °C or lower. Only with compounds **4**, **9**, and **14** were clear decoalescences observed below ca. -20 °C with the appearance of two sets of signals, corresponding to two rotamers with rather unequal populations (Table VII). In the spectra of compounds **2** and **8**, some signals

(38) Sundaralingam, M. *Biopolymers* **1969**, 7, 821–860.(39) Berg, U.; Grimaud, M.; Sandström, J. *Nouv. J. Chim.* **1979**, 3, 175–181.(40) Berg, U.; Liljefors, T.; Roussel, C.; Sandström, J. *Acc. Chem. Res.* **1985**, 18, 80–86.(41) Jaime, C.; Osawa, E. *J. Chem. Soc., Perkin Trans. 2* **1984**, 995–999.(42) (a) Manoharan, M.; Eliel, E. L. *J. Am. Chem. Soc.* **1984**, 106, 367–372. (b) Pettersson, I.; Berg, U. *J. Chem. Soc., Perkin Trans. 2* **1985**, 1365–1375.(43) Allinger, N. L. *Adv. Phys. Org. Chem.* **1976**, 13, 17.(44) Pèpe, G.; Pierrot, M. *Acta Crystallogr., Sect. B: Struct. Crystallogr. Cryst. Chem.* **1976**, B32, 1317–1320, 1321–1325.

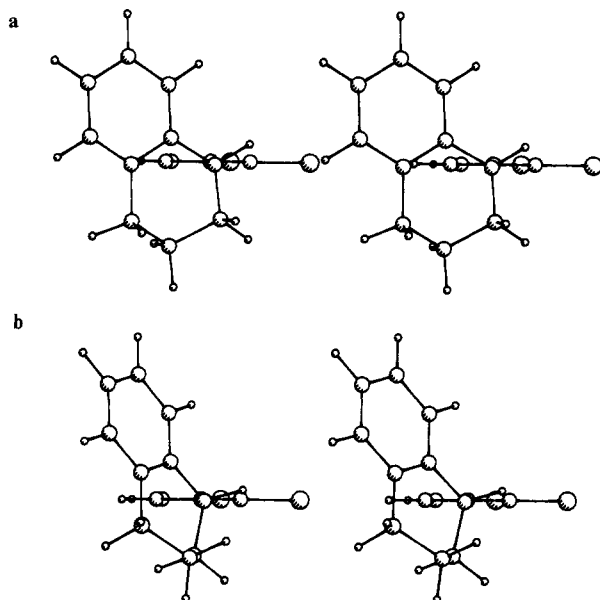


Figure 4. Stereoscopic view of **12** with (a) anti axial and (b) anti equatorial conformation.

Table VII. Free Energies of Activation, Populations, and Free Energy Differences for the syn \rightarrow anti Exchange in **4**, **9**, and **14**^a

compd	temp, °C	ΔG^\ddagger , kcal/mol	P_{syn}^b	ΔG° , kcal/mol
4	-10	11.9	0.123	-1.03
	-37	11.6	0.100	-1.03
	-62	11.6	0.079	-1.03
9	+6	12.0	0.088	-1.24
	-37	12.1	0.066	-1.24
	-61	12.3	0.053	-1.22
14	+11	14.1	0.161	-0.93
	+4.5	14.0	0.156	-0.93
	-13	13.8	0.142	-0.93

^a Solvent (CD₃)₂O. ^b Fractional population.

were strongly broadened in the temperature region just below ambient, but became sharp again at lower temperatures, indicating that an exchange between two rotamers in a strongly biased equilibrium becomes slow on the NMR timescale.

In the previous studies of three-substituted thiazoline-2-thiones^{7,8} and of similar acyclic thioamides,⁹ the resonance of the rotor methine (H_α) of the anti form was regularly observed 1.2–1.4 ppm downfield of that of the syn form, due to the strong deshielding effect of the thiocarbonyl group in the sp^2 plane.⁴⁵ In compound **4**, the difference is ca. 1.7 ppm (Table VIII), and in **9** and **15** it is 1.9–2.0 ppm, with the resonance of the major form at lower field (ca. δ 7). The larger difference in the 3-(1-phenylethyl) derivatives is probably due to extra shielding of H_α in the syn form by the 4-Ph group.

These observations lead to the conclusion that the major rotamer in **4**, **9**, and **14** is the anti form, and furthermore that this form dominates even more (>99%) in the other compounds with sterically less demanding 4-substituents, since here the H_α resonance invariably is found in the region δ 6.5–7.2.

The assignment of the dominant rotamer to the anti form is supported by other striking chemical shift effects. In this rotamer, the phenyl group of the rotor is ideally placed to exert a strong shielding effect on the substituent in position 4 of the thiazoline-2-thione ring. Thus the 4-methyl ¹H resonance in **2**, **6**, and **12** appears at δ 1.80, 1.75, and 1.78, respectively, whereas the corresponding shifts for the syn and anti forms of the 3-isopropyl analogue of **2** are 2.25 and 2.42, respectively.³² The 4-isopropylmethyl resonances in **3** and **8** appear as doublets of doublets

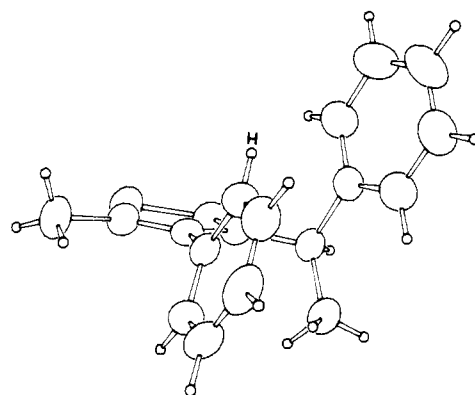


Figure 5. ORTEP drawing of **9**.

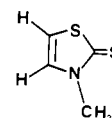
with one of these at unusually high field (δ 0.55–0.57, Table VIII). The other isopropyl methyl resonances appear at δ 1.16 and 1.20 and the CH septets at δ 2.73 and 2.85, respectively. These values should be compared with δ 1.12 and 1.20 for the doublets and δ 3.32 and 3.59 for the septets of the *N*-4-diisopropyl analogue of **3**.³² This strong shielding is in agreement with the expected approximately bisected orientation of the 4-isopropyl group with respect to the thiazolinethione ring, in which one isopropyl methyl group will be much closer to the face of the benzene ring than the other.

The 4-phenyl groups in **9** and **14** rotate slowly on the NMR timescale already at ambient temperature, and when the rotation of the *N*-substituent is slow at ca. -30° , a doublet with *J* ca. 8 Hz and with additional fine structure appears at δ 5.7–5.9, which integrates for one proton in the major rotamer. The same phenomenon is observed for **4** below -70°C . This doublet is clearly due to the proton marked H in Figure 5. The free energy barriers to rotation of the 4-phenyl group in **4**, **9**, and **14** were found to be 9.4, 15.9, and 15.2 kcal/mol, respectively, the higher barriers in the two latter compounds (in toluene-*d*₈) evidently being due to hindrance by the 5-methyl group.

The rotor methyl ¹H resonances of the major rotamers of **4** and **9** appear at 0.6–0.7 ppm higher field than for the minor form. In this case the extra shielding is provided by the 4-phenyl ring in the anti form.

The aromatic solvent induced shift (ASIS)⁴⁶ method has previously been useful in the assignment of resonances to syn and anti rotamers.⁷ This technique is based on the observation that nuclei close to the positive end of a dipolar molecule are considerably more shielded in an aromatic solvent than in, e.g., chloroform, whereas nuclei close to the negative end, the thiocarbonyl sulfur atom, are only slightly shielded or even deshielded. From CDCl₃ to toluene-*d*₈ the rotor methyl proton resonances in **1** and **2** underwent upfield shifts of 0.49 and 0.47 ppm, respectively, whereas the H_α resonance was shifted by only 0.05 and 0.02 ppm, both results in agreement with a dominant anti form. The corresponding shift for Me-4 in **2** is 0.49 ppm, and H4 and H5 in **1** are shifted by 0.90 and 0.84 ppm, all in good agreement with preferential solvation of the positive end of the molecular dipole by the toluene molecules.

A strong temperature effect on $\delta(H4)$ is observed for **1**, **5**, **10**, and **12**, and a somewhat smaller effect on $\delta(H5)$ in **1** and **2**, all in (CD₃)₂O solution (Table VIII). This is not due to a concentration effect, since the shifts are independent of the concentration over a 120 °C interval in 8.1, 60, and 330 mM solutions. The *N*-methyl analogue of **1** (**15**) shows a similar effect, although the



15

(45) Walter, W.; Schaumann, E.; Paulsen, H. *Justus Liebigs Ann. Chem.* **1969**, 727, 61–70.

(46) Laszlo, P. *Prog. Nucl. Magn. Reson. Spectrosc.* **1967**, 3, 231–402 and references therein, in particular ref 329 and 330.

Table VIII. ^1H Chemical Shifts (δ) for **1–14**

compd	solvent	temp, °C	H_a^a	CH_3^a	R^4	R^5
1	$(\text{CD}_3)_2\text{O}$	+24	6.586	1.704	7.002	6.568
		−60.5	6.567	1.712	7.218	6.735
		−139	6.555	1.737	7.541	6.944
2	$(\text{CD}_3)_2\text{O}$	+23	7.153	1.762	1.800	6.209
		−72.5	7.124	1.782	1.782	6.395
		−122	7.088	1.79 ^b	1.78 ^b	6.496
		−144	7.079	1.79 ^b	1.78 ^b	c
3	CDCl_3	+30	c	1.859	0.572 (d), 1.162 (d), 2.726 (sept)	6.216
4	CDCl_3	+30	c	1.628		6.305
5	$(\text{CD}_3)_2\text{O}$	−58	7.01, ^d 5.33 ^e	1.475, ^d 2.151 ^e	f	6.56 ^d
		−126	6.97, ^d 5.32 ^e	1.420, ^d 2.191 ^e	5.576 ^g	6.82 ^d
		+24	6.560	1.676	6.682 (q, $J = 1.40$ Hz)	2.069 (d, $J = 1.40$ Hz)
		−64	6.538	1.681	6.890	2.089
6	CDCl_3	+30	6.513	1.694	7.114	2.107
		+30	6.545	1.722	6.560 (q, $J = 1.40$ Hz)	2.116 (d, $J = 1.40$ Hz)
		+30	c	1.834	1.750	2.054
7	CDCl_3	+30	c	1.840	0.584 (t), 2.339 (q)	2.073
8	CDCl_3	+30	7.235	1.816	0.551 (d), 1.203 (d), 2.854 (sept)	2.168
9	CDCl_3	+30	f	1.581		6.305
10	$(\text{CD}_3)_2\text{O}$	−33	7.05, ^d 5.09 ^e	1.469, ^d 2.074 ^e	5.936 ^g	1.767, ^d 1.993 ^e
		−118	6.976, ^d 5.080 ^e	1.418, ^d 2.100 ^e	5.754 ^g	
		+24	6.632	1.772	7.310	
11	CDCl_3	−61	6.622	1.788	7.649	
		−141	6.604	1.874	8.036	
		+30	c	1.900	1.884	
12	$(\text{CD}_3)_2\text{O}$	+22	6.45 ^h		6.78	6.54
		−74	6.44		7.06	6.75
		−131	6.45		7.35	6.93
13	$(\text{CD}_3)_2\text{O}$	−47	7.035 ^{i,j}		1.781 (d, $J = 1.2$ Hz)	6.358 (q, $J = 1.2$ Hz)
14	$(\text{CD}_3)_2\text{O}$	−40	7.040, ^{d,k} 5.015 ^{e,l}		5.730 ^g	1.798, ^d 1.994 ^e
		−92	7.020, ^{d,k} 5.014 ^{e,l}		5.717 ^g	1.825, ^d 2.019 ^e
15	$(\text{CD}_3)_2\text{O}$	+21	3.575 ^m		6.588	7.109
		−58	3.568		6.725	7.260
		−121	3.555		6.835	7.392

^a In rotor. ^b Broad, overlapping doublets. ^c Hidden by aromatic resonances. ^d Major rotamer. ^e Minor rotamer. ^f Strongly broadened. ^g Doublet (J ca. 7.5 Hz) with fine structure, corresponding to one aromatic proton in the major rotamer. ^h Doublet of doublets with $J_+ = 13.6$ Hz. ⁱ Doublet of doublets with $J_+ = 18.0$ Hz. ^j The protons in the saturated part of the tetrahydronaphthalene part (Scheme II) were assigned by COSY experiment: a, b at δ 1.9 and 2.3, c, d at 1.9 and 2.1, e, f at 2.85. ^k Doublet of doublets with $J_+ = 19.5$ Hz. ^l Doublet of doublets with $J_+ = 17.7$ Hz. ^m N-Methyl protons.

shift of H4 is less than for **1**. The shift displayed by **15** may be due to a temperature-dependent solute-solvent interaction, but the excess deshielding of H4 in **1**, **5**, and **10** with descending temperature is better explained by shifts in equilibria between two conformers of the anti type, as suggested by MM calculations (Figure 2), the conformer with least shielded H4 being energetically favored. In contrast to $\delta(\text{H4})$ and $\delta(\text{H5})$, $\delta(\text{H}_a)$ is remarkably temperature-insensitive.

The methine proton in the tetrahydronaphthalene derivatives **12–14** form the X part of an ABCDEFX spin system. This resonance, which appears as a doublet of doublets, can be treated as the X part of an ABX system;⁴⁷ i.e., the splitting between the outer lines, J_+ , is equal to $|J_{AX} + J_{BX}|$. J_+ contains stereochemical information, since J_{AX} and J_{BX} are the vicinal couplings, and a high J_+ value indicates a large proportion of pseudoequatorial forms with vicinal couplings in one antiperiplanar and one gauche related pair of protons. A low J_+ value, on the other hand, indicates a large proportion of pseudoaxial forms with two gauche couplings. The temperature dependence of J_+ is too indistinct to give any information, but it is obvious that **12**, with $J_+ = 14$ Hz, contains more of the pseudoaxial forms than **13** and **14** with $J_+ = 18$ and 19.5 Hz, respectively, in agreement with the MM calculations (Table VI).

The free energy barriers to syn \rightarrow anti rotation in **4**, **9**, and **14** are 12–14 kcal/mol (Table VII). The syn \rightarrow anti barrier in the *N*-(1-(methoxycarbonyl)ethyl) analogue of **9** has been measured to 13.3 kcal/mol.⁴⁸ Thus the steric requirements of the 1-phenylethyl and the 1-(methoxycarbonyl)ethyl groups in the transition state seem to be rather similar. The ca. 2 kcal/mol higher barrier for **14** can be ascribed to the more rigid rotor. A

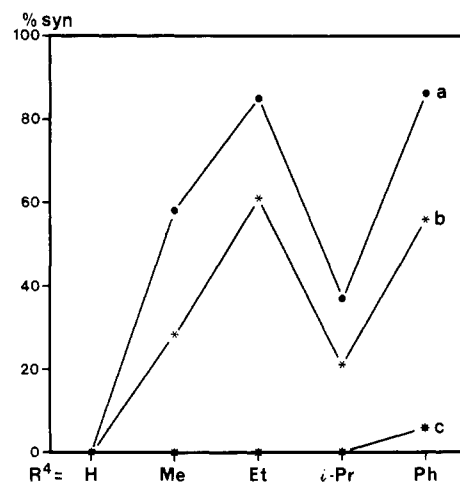


Figure 6. Percent syn form, recalculated to -50°C , for thiazoline-2-thiones with $\text{R}^3 = \text{CH}_3\text{CHX}$, $\text{R}^5 = \text{CH}_3$: (a) $\text{X} = \text{CO}_2\text{CH}_3$; (b) $\text{X} = \text{CH}_3$; (c) $\text{X} = \text{Ph}$. Solvent for (a) and (b) acetone- d_6 , except when $\text{R}^4 = \text{Ph}$, in all other cases dimethyl ether- d_6 .

similar difference (1.5 kcal/mol) is found between *N*-isopropyl- and *N*-cyclohexylthiazoline-2-thiones.⁷

While the barriers for the three classes of thiazolinethiones (**I**, $\text{R} = \text{Me}$, CO_2Me , and Ph) show no unexpected differences, the rotamer populations do (Figure 6). While the syn form becomes important in the first two classes already when $\text{R}^4 = \text{Me}$, the anti form is strongly favored for all 1-phenylethyl derivatives. This is not predicted by the MM calculations, and we cannot at present decide if the rotamer preference is caused by a specific repulsion between the thiocarbonyl sulfur atom and the rotor benzene ring

(47) Nilsson, I. Thesis, University of Lund, 1985.

(48) Roschester, J.; Berg, U.; Sandström, J., to be published.

Table IX. Ultraviolet Spectra of 1-14

compd	solvent	λ_{\max} , nm (ϵ)	λ_{\max} , nm (ϵ)	λ_{\max} , nm (ϵ)
1	MeOH	315.5 (18 000)		202.3 (28 000)
	CH ₂ Cl ₂	319.4 (16 500)		
	hexane	320.1 (16 300)	227 (sh, 7100)	201.9 (26 500)
	EPA ^a	317.5 (13 800)		205.9 (23 600)
2	MeOH	320.3 (14 800)		201.9 (25 100)
	CH ₂ Cl ₂	323.7 (15 600)		
	hexane	324.8 (16 900)	231.6 (8700)	206.9 (28 000)
	EPA	321.7 (15 700)		
3	MeOH	321.2 (16 500)		201.0 (27 200)
	CH ₂ Cl ₂	323.6 (18 100)		
	hexane	325.1 (16 200)	233 (9200)	207.6 (25 300)
	EPA	323.3 (15 200)		207.0 (23 200)
4	MeOH	321.0 (18 300)		
	hexane	324.1 (17 200)		
	EPA	322.6 (21 800)		
5	MeOH	319.4 (17 800)		202.5 (28 800)
	hexane	322.0 (23 900)		207.1 (35 300)
6	MeOH	324.5 (15 500)	216 (sh, 18000)	202.6 (25 800)
	hexane	327.4 (15 600)	235.0 (7300)	207.5 (22 800)
	EPA	325.5 (19 500)	227 (sh, 12000)	206.7 (29 000)
7	MeOH	325.5 (15 400)	217 (sh, 16800)	202.5 (24 700)
	hexane	328.9 (18 100)	235.8 (8600)	208.0 (25 400)
	EPA	326.8 (16 200)	230 (sh, 10000)	206.9 (23 600)
8	MeOH	324.2 (15 800)	217 (sh, 17000)	202.5 (25 500)
	CH ₂ Cl ₂	327.2 (17 500)		
	hexane	327.8 (16 700)	236.9 (8100)	208.0 (23 500)
	EPA	325.3 (18 200)	227 (sh, 10000)	206.5 (26 000)
9	MeOH	324.2 (16 100)		
	CH ₂ Cl ₂	327.5 (16 800)	250 (sh, 6000)	
	hexane	327.8 (15 500)	255 (sh, 5500)	
	EPA	326.9 (15 500)	246 (sh, 6000)	
10	MeOH	342.1 (27 100)	289 (sh, 3700)	217.5 (sh, 29 100)
	CH ₂ Cl ₂	343.7 (23 800)		
	hexane	346.2 (26 400)	290 (3800) sh at 240, 234 (13000, 14000)	
	EPA	sh at 356 (22 300) 343.6 (23 200)		218 (sh, 23 000)
11	MeOH	332.9 (18 900)		215 (sh, 23 900)
	CH ₂ Cl ₂	336.6 (20 400)		
	hexane	337.2 (21 000)	232 (sh, 13700)	
12	MeOH	314.5 (16 500)		206 (sh, 31 000)
	hexane	319.1 (15 800)	228 (sh, 8000)	208.4 (28 600)
	EPA	317.5 (15 800)		207.0 (28 000)
13	MeOH	319.2 (16 000)		203 (35 000)
	hexane	322.5 (15 700)	230 (sh, 8000)	209 (29 500)
	EPA	321.9 (16 000)	227 (sh, 12000)	207.6 (30 700)
14	MeOH	323.4 (15 500)		
	hexane	327.4 (16 200)		
	EPA	326.0 (17 400)		

^a Diethyl ether:isopentane:ethanol (5:5:2, v/v).

or by an attraction between this ring and the 4-substituent, or by some other effect.

Ultraviolet Spectra. The simple thiazoline-2-thione chromophore displays a strong absorption band in the region around 320 nm (ϵ 15,000–20,000). It has been assigned by PPP⁶ and CNDO/S⁴ calculations to a $\pi \rightarrow \pi^*$ transition. Besides, a shoulder is observed at 250 nm and a stronger band (ϵ ca. 5000) at 215 nm, both assigned to $\pi \rightarrow \pi^*$ transitions.⁴ An $n \rightarrow \sigma^*$ transition is calculated to give absorption between 250 and 320 nm, but it is not assigned to a band in the spectrum.⁴ In compounds 1–14, the N-substituent gives rise to absorption around 260 (weak, with vibrational fine structure) and at 200–210 nm due to transitions to the ¹L_b and ¹L_a states of the benzene ring, respectively.⁴⁹ In the spectra of 4, 9–11, and 14, the thiazolinethione transitions

are modified by conjugation with phenyl rings in positions 4 or 5.

In all cases, an $n \rightarrow \pi^*$ transition in the thiocarbonyl group is expected, and it is calculated to have lower energy than the first $\pi \rightarrow \pi^*$ transition.⁴ However, no corresponding band is observed, in all likelihood because it is hidden below the strong absorption band with maximum near 320 nm. The UV spectral data of compounds 1–14 are given in Table IX.

As has been observed earlier,⁵⁰ the bathochromic effect of phenyl substitution on the first $\pi \rightarrow \pi^*$ transition is larger in position 5 than in position 4. The bathochromic effect is particularly large in 10, where coplanarity of the two rings is possible. Alkyl substitution also has a general bathochromic effect in positions 4 and 5. In the series 6, 7, and 8 we observe the same

(49) Platt, J. R. *J. Chem. Phys.* **1949**, *17*, 484–495.(50) Kjellin, G.; Sandström, J. *Acta Chem. Scand.* **1969**, *23*, 2888–2899.

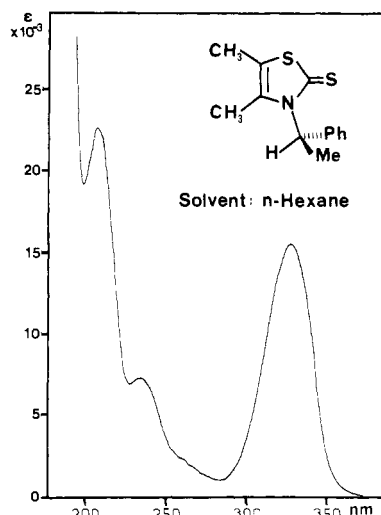


Figure 7. UV spectrum of **6** in hexane.

drop in λ_{\max} for the 4-*i*-Pr derivative **8** as was observed for the 3-*i*-Pr and 3-cyclohexyl analogues, which was ascribed to static gearing and to differences in strain between the ground state and the excited state in the two rotamers corresponding to syn **I** and anti **I**.⁵ However, the consistent dominance of the anti form in all of **6**, **7**, and **8** renders this explanation invalid for the 3-phenylethylthiazoline-2-thiones.

The absorption band displayed by **1**–**3** and **6**–**8** at 227–237 nm in hexane (Figure 7) probably originates in a $\pi \rightarrow \pi^*$ transition in the thiazoline-2-thione chromophore. It undergoes a blueshift and appears as a shoulder at ca. 217 nm in MeOH. The band at ca. 320 nm, assigned to the first $\pi \rightarrow \pi^*$ transition in the same chromophore, is shifted by 3–4 nm to shorter wavelength from hexane to MeOH, in agreement with a calculated (CNDO/S) charge displacement from the thiocarbonyl sulfur atom in this transition.

The temperature-dependent CD spectra will be discussed for the *R* configuration with EPA (see Table IX) as the standard solvent. Wavelengths and $\Delta\epsilon$ values for extrema are given in Table X. The compounds can be subdivided into three main groups: (1) Compounds **1**, **5**, and **10**, all without substituent in position 4, show a weak negative band (band 1) around 340 nm (370 nm for **10**) and a positive band (band 2) in the region 310–320 nm (330–340 nm for **10**). Both bands increase considerably in strength (Figure 8) with decreasing temperature. (2) Compounds **12** and **13** show strong positive bands 1 and negative bands 2 (Figure 9). With decreasing temperature, both bands decrease in intensity in **12**, to the extent that band 2 disappears at -150°C (Figure 9a), whereas in **13** both bands increase in intensity (Figure 9b). (3) The remaining compounds display only one band (positive) in the region above 300 nm. In all nonphenyl substituted compounds this band is mainly composed of band 1, band 2 even being slightly negative at low temperature in **2**, **6**, and **8** (Figure 10). In **4**, **9**, **11**, and **14** bands 1 and 2 both contribute significantly, and in all compounds in the group, band 1 increases more or less in intensity with decreasing temperature.

At shorter wavelengths, the CD spectra of the three groups are more similar, displaying a weak positive band with vibrational fine structure at 260–270 nm (band 3), a strong negative band at 230–240 nm (band 4), and an even stronger positive band near 210 nm (band 5). In some cases it was also possible to observe a strong negative band at shorter wavelength. The 4- and 5-phenyl-substituted compounds also display a new negative band in the region 280–300 nm (within brackets in Table X), the intensity of which increases strongly with decreasing temperature (Figure 11).

Based on CNDO/S calculations and a notable blueshift with increasing solvent polarity (Table X), band 1 is assigned to the $n \rightarrow \pi^*$ transition in the thiazoline-2-thione chromophore. Band resolution shows band 2 to fall at the position of the first strong UV band, and it is assigned to the first strong $\pi \rightarrow \pi^*$ transition

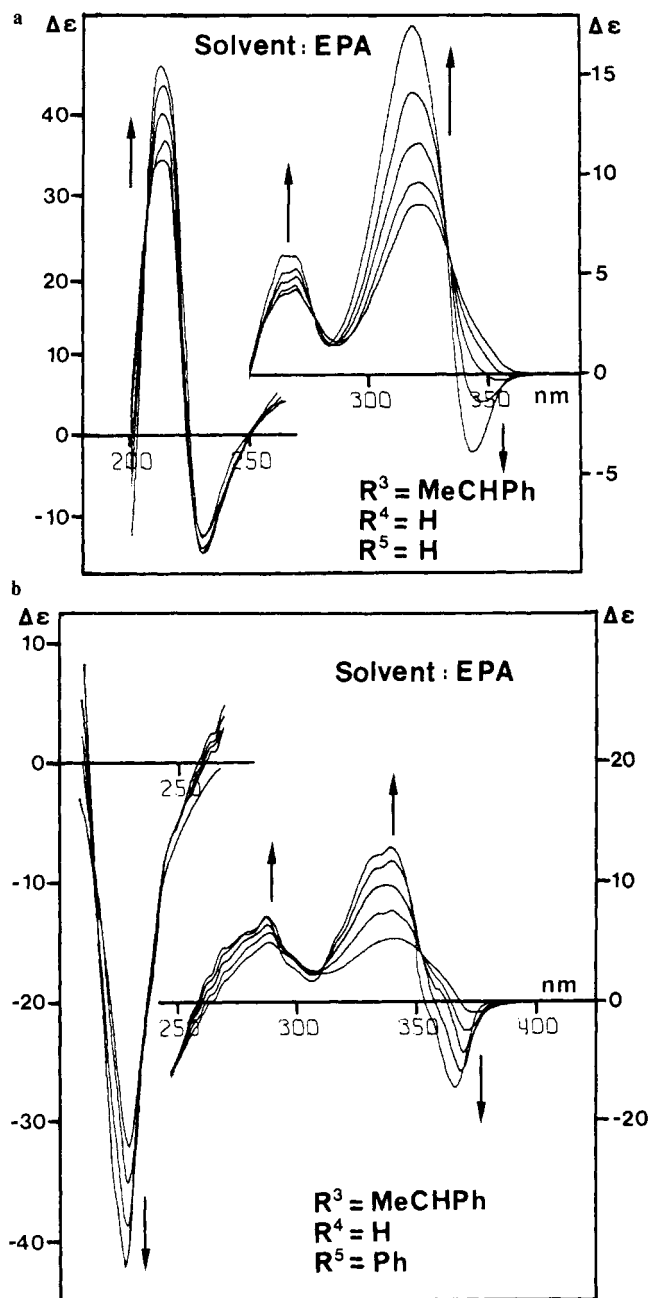


Figure 8. (a) CD spectra of **1** in EPA at +22, -26, -65, -105, and -148 $^\circ\text{C}$; (b) CD spectra of **10** in EPA at +22, -27, -66, -110, and -156 $^\circ\text{C}$ (-151°C for short wavelength section). The arrows indicate lowered temperature.

in the same chromophore. Band 3 is assigned to the transition to the $^1\text{L}_b$ state of the benzene chromophore, and band 4 to a $\pi \rightarrow \pi^*$ transition in the thiazolinethione chromophore. Band 5 is most likely due to the $^1\text{L}_a$ transition in the benzene chromophore, shifted to longer wavelength by overlap with the negative band at shorter wavelength. Bands 4 and 5 in compounds **1**–**11** are much less dependent on solvent, substituents, and temperature than bands 1 and 2. This is not unexpected, since the rotational strengths of the corresponding transitions must have important contributions from the coupled oscillator mechanism involving the benzene $^1\text{L}_a$ transition. The direction of the moment of this transition is independent of the angle of rotation of the benzene ring (ϕ_2). Therefore, the sign of this "couplet" has been used to assign the configurations of compounds **12**–**14**.

The CD spectra of several of the compounds show strong temperature dependence, and the spectra intersect in isosbestic points, indicating temperature-dependent equilibria between pairs of conformational isomers. An alternative explanation in terms

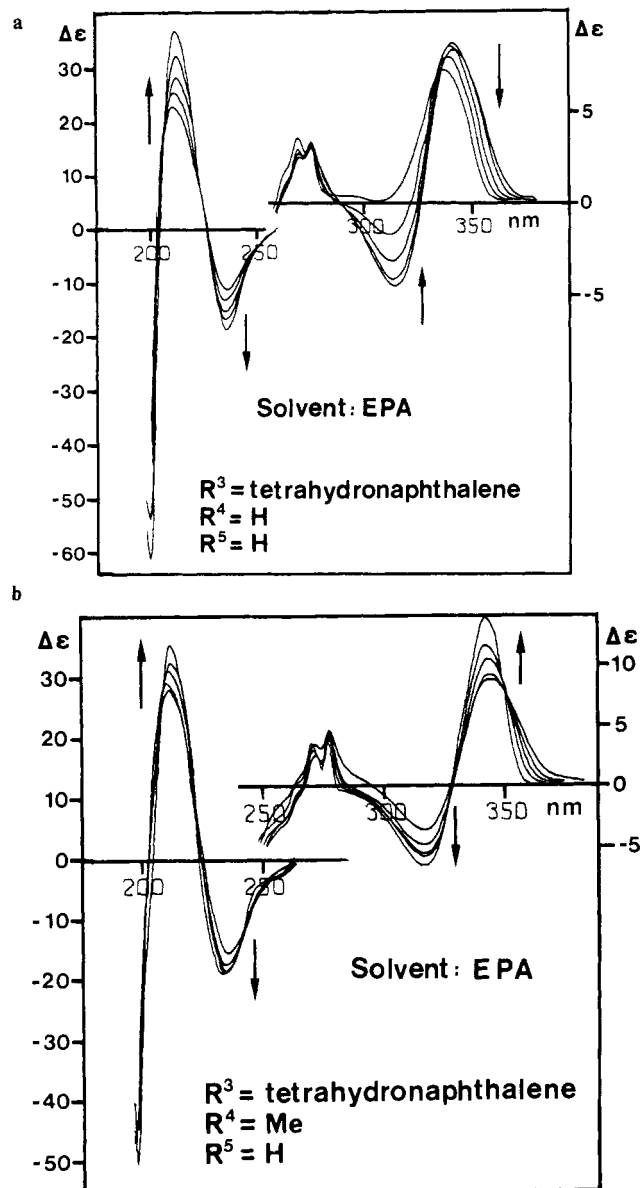


Figure 9. (a) CD spectra of **12** in EPA at +19 (+21), -25, -71, -109 (-111), -151 (-158) °C; (b) CD spectra of **13** in EPA at +20 (+22), -24 (-27), -72 (-79), -110 (-115), -175 °C. Temperatures in parentheses refer to short wavelength region, when different from those for long wavelength region.

of solvent effects is much less likely. The $n \rightarrow \pi^*$ bands of carbonyl groups may appear with different signs in solvated and unsolvated forms,⁵⁰ but as expected the maxima differ considerably in wavelength, which is not the case with the thiazolinethiones, for which the differences in $\Delta\epsilon$ are an order of magnitude or more larger than for the ketones. Since analysis of NMR spectra unequivocally shows strong (>99%) dominance of the anti form except for the 4-phenyl compounds **4**, **9**, and **14** (Table VII), the isomers must both be of the anti type, and the exchange between them must be fast on the NMR timescale down to -140 °C.

The spectra of **1** in the region 280–380 nm (Figure 8a) are well reproduced by two Gaussians with opposite signs, centered at 319 and 340 nm and with exponential halfwidths, Δ , of 24 and 13 nm. The apparent rotational strengths, R_{app} , were evaluated in Debye-Bohrmagneton (D·BM)⁵² by the expression $R_{app} = 0.2476 \cdot \Delta \cdot \Delta\epsilon \cdot \sqrt{\pi/\lambda_{max}}$. This operation was performed at several

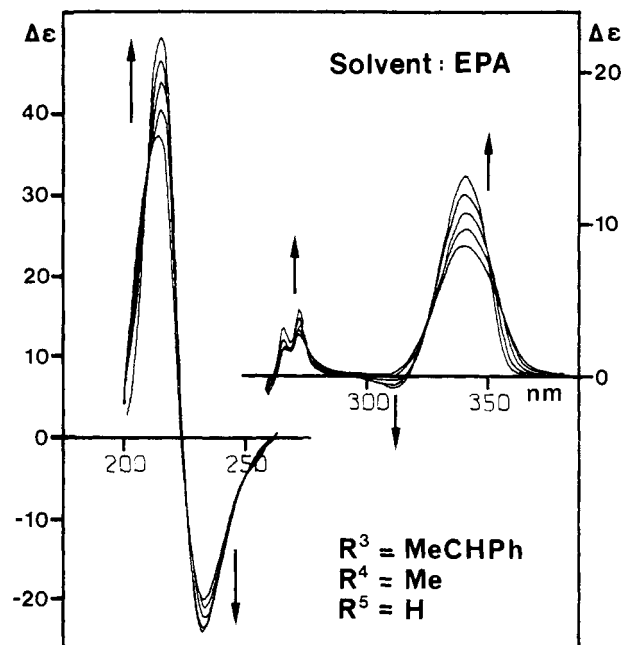


Figure 10. CD spectra of **2** in EPA at +21, -23, -65, -110, and -149 °C.

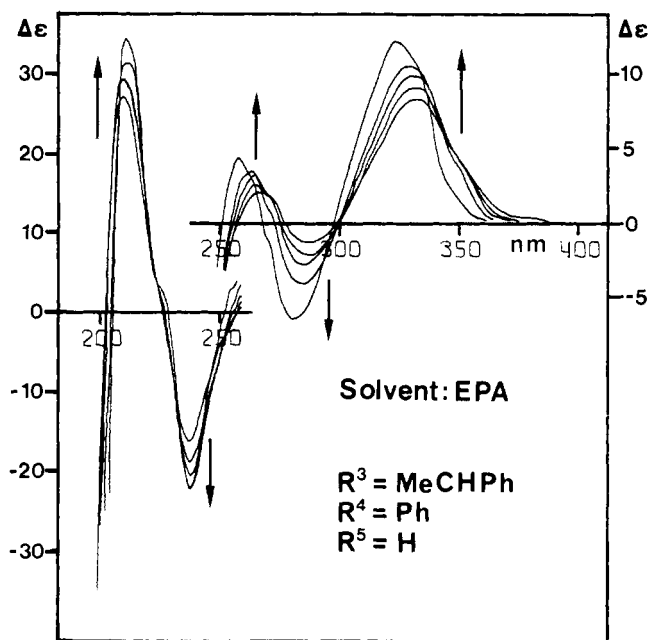


Figure 11. CD spectra of **4** in EPA at +21, -25, -65, -112, and -163 (-158) °C.

temperatures, and the free-energy extrapolation method described by Wood et al.^{53a} and by Moscovitz et al.^{53b} was employed to find the ΔG° value and the R values for the individual forms (Table XII). It is instructive to compare the rotational strengths for the compounds from group 1 with those from group 3, notably **2**, **6**, and **8**. In the first group we have a major rotamer with negative $n \rightarrow \pi^*$ and positive $\pi \rightarrow \pi^*$ bands and a minor rotamer with opposite signs. For the major rotamers of **2**, **6**, and **8**, the signs are as for the minor ones from group 1. The MM calculations give two energy minima in the anti forms of **1** and **2**, with rather similar geometries, and equivalent results should be expected for all compounds of groups 1 and 3. For both systems, the

(51) Rassat, A. In *Optical Rotatory Dispersion and Circular Dichroism in Organic Chemistry*; Sznatzke, G., Ed.; Heyden & Son: London, 1967; pp 314–328.

(52) 1 D·BM = $3.0917 \cdot 10^{-53} \text{ A}^2 \text{ m}^3 \text{ s} = 3.2742 \cdot 10^{-39} \text{ cgs units}$.

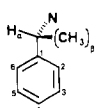
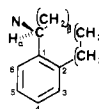
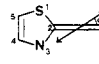
(53) (a) Wood, W. W.; Fickett, W.; Kirkwood, J. G. *J. Chem. Phys.* **1952**, *20*, 561–568. (b) Moscovitz, A.; Wellman, K.; Djerassi, C. *J. Am. Chem. Soc.* **1963**, *85*, 3515–3516. (c) Joshua, H.; Gans, R.; Mislow, K. *J. Am. Chem. Soc.* **1968**, *90*, 4884–4892.

Table X. CD Spectra of 1-14 λ_{max} or λ_{min} , nm ($\Delta\epsilon$ cm⁻¹ M⁻¹)

compd	solvent	temp, °C	band 1	band 2	band 3	band 4	band 5
(R)-1	MeOH	22	348 (-0.56)	315 (-9.2)	262 (+3.5)	232 (-8.1)	212 (+22.8)
		-82	344 (-1.54)	314 (+12.1)	261 (+4.5)	231 (-10.3)	213 (+30.1)
	CH ₂ Cl ₂	22	355 (-0.04)	324 (+7.8)	268 (+3.5)	234 (-9.7)	
	hexane	22	337 (+5.0) ^a		271 (+4.2)	231 (-13.8)	215 (+34.2)
	EPA	22	366 (-0.083)	321 (+7.6)	269 (+3.9)	230 (-12.6)	214 (+32.3)
		-147	343 (-4.0)	318 (+17.4)	269 (+5.9)	230 (-12.9)	214 (+45.8)
(R)-2	MeOH	23	334 (+7.7)		270 (+1.5)	231 (-18.0)	211 (+27.3)
		-85	336 (+9.8)		270 (+2.5)	231 (-21.5)	214 (+35.5)
	CH ₂ Cl ₂	22	339 (+9.3)	305 (-0.3)	271 (+1.9)	234 (-18.1)	
	hexane	22	346 (+7.9)	312 (-0.6)	273 (+3.1)	234 (-18.9)	215 (+42.3)
	EPA	21	347 (+8.4)		272 (+2.8)	233 (-20.3)	215 (+39.5)
		-150	340 (+13.2)	313 (-0.8)	272 (+4.4)	232 (-25.2)	216 (+48.8)
(R)-3	MeOH	22	334 (+7.4)		271 (+1.6)	233 (-15.1)	215 (+26.3)
	hexane	22	346 (+8.2)		274 (+3.0)	236 (-22.6)	218 (+50.5)
	EPA	21	340 (+7.8)		272 (+2.0)	234 (-21.7)	217 (+37.9)
		-177	341 (+11.6)		271 (+4.0)	232 (-24.4)	218 (+45.1)
(R)-4	MeOH	22	328 (+7.5)	[282 (-1.2)] ^b	264 (+1.3)	235 (-12.7)	212 (+26.4)
	CH ₂ Cl ₂	22	334 (+7.7)	[287 (-1.8)] ^b	265 (+2.7)	238 (-13.2)	
	hexane	22	336 (+6.4)	[291 (-6.1)] ^b	270 (+3.0)	240 (-11.6)	209 (+20.8)
	EPA	21	332 (+8.2)	[286 (-1.4)] ^b	267 (+2.1)	238 (-17.4)	210 (+27.0)
		-162	324 (+12.1)	[282 (-6.5)] ^b	259 (+4.4)	237 (-22.1)	211 (+34.1)
	(R)-5	MeOH	23	349 (-0.7)	317 (+8.6)	261 (+1.9)	232 (-8.0)
-83			346 (-1.5)	317 (+11.1)	263 (+2.4)	233 (-10.9)	
CH ₂ Cl ₂		22	354 (-0.44)	323 (+8.2)	270 (+2.0)	235 (-8.8)	216 (+25.1)
hexane		24	338 (+6.3) ^a		271 (+2.5)	231 (-10.8)	216 (+28.4)
		-51	339 (+7.8) ^a		271 (+2.5)	230 (-11.8)	215 (+33.9)
		21	336 (-0.30)	325 (+7.0)	271 (+2.1)	232 (-9.8)	217 (+27.3)
EPA		-157	334 (-5.4)	321 (+13.9)	270 (+3.5)	231 (-12.3)	214 (+40.7)
		(R)-6	MeOH	22	335 (+7.8)		271 (-1.1)
hexane	22		347 (+8.3)		278 (+1.2)	238 (-16.2)	216 (+37.5)
EPA	22		343 (+8.2)		272 (+0.9)	235 (-19.0)	216 (+35.5)
	-174		344 (+13.9)	311 (-0.5)	272 (+2.6)	234 (-25.6)	216 (+45.5)
(R)-7	MeOH	22	336 (+7.1)		271 (+1.2)	234 (-14.5)	216 (+25.5)
	hexane	22	346 (+8.3)		273 (+1.4)	239 (-17.6)	218 (+42.4)
	EPA	23	342 (+8.5)		273 (+1.4)	234 (-19.6)	218 (+38.4)
		-161	345 (+13.8)		271 (+1.9)	233 (-24.9)	218 (+49.0)
(R)-8	MeOH	22	336 (+8.5)		271 (+1.2)	234 (-18.6)	216 (+32.1)
	CH ₂ Cl ₂	22	340 (+9.5)		273 (+0.9)	237 (-19.4)	218 (+34.9)
	hexane	22	347 (+11.1)		282 (+1.1)	241 (-20.5)	219 (+56)
	EPA	21	343 (+8.6)		273 (+1.1)	236 (-18.0)	217 (+39.0)
		-174	344 (+14.6)	315 (-1.3)	272 (+2.6)	235 (-24.0)	218 (+46.3)
	(R)-9	MeOH	21	333 (+8.3)	[285 (-1.1)] ^b	265 (+1.2)	236 (-1.63)
-87			334 (+10.0)	[285 (-2.2)] ^b	264 (+1.9)	236 (-22.3)	211 (+28.9)
CH ₂ Cl ₂		22	338 (+8.5)	[288 (-1.9)] ^b	266 (+1.4)	238 (-13.8)	
hexane		22	343 (+7.9)	[293 (-1.0)] ^b	273 (+0.9)	238 (-12.0)	209 (+22.5)
EPA		22	339 (+8.3)	[290 (-0.8)] ^b	271 (+1.8)	236 (-15.4)	
		-145	339 (+9.7)	[288 (-3.7)] ^b	270 (+1.3)	236 (-21.6)	
(R)-10	MeOH	25	368 (-1.7)	329 (+6.4)	[286 (+3.1)] ^b	226 (-24.1)	
		-81	366 (-4.5)	331 (+9.3)	[286 (+4.9)] ^b	224 (-30.8)	
	CH ₂ Cl ₂	22	372 (-0.5)	339 (+3.1)	[288 (+2.6)] ^b		
	hexane	25	366 (+6.2)	330 (-0.37)	[290 (+5.1)] ^b	229 (-31.2)	214 (sh, -4.5)
		-32	367 (+9.0)	331 (-1.23)	[290 (+5.5)] ^b		
		22	373 (-1.0)	341 (+5.3)	[289 (+5.0)] ^b	227 (-32.2)	
	EPA	-156	368 (-7.3)	340 (+12.8)	[288 (+7.2)] ^b	227 (-42.3)	
		(R)-11	MeOH	22	345 (+6.8)	[291 (+2.8)] ^b	271 (+1.8)
CH ₂ Cl ₂	22		348 (+7.7)	[295 (+3.1)] ^b	272 (+1.2)	233 (-22.3)	
(R)-12	MeOH	22	334 (+7.5)	306 (-3.3)	268 (+2.2)	234 (-9.5)	212 (+174)
	hexane	22	348 (+9.1)	317 (-7.8)	277 (+3.6)	236 (-12.2)	211 (+22.6)
	EPA	19	342 (+8.4)	317 (-4.6)	271 (+3.2)	234 (-12.1)	212 (+22.8)
		-150	337 (+7.3)	308 (0.0)	269 (+3.7)	234 (-17.9)	213 (+36.5)
(R)-13	MeOH	22	338 (+8.7)	309 (-4.2)	276 (+2.5)	234 (-14.3)	210 (+23.4)
	hexane	22	349 (+9.0)	320 (-6.1)	278 (+5.6)	237 (-19.6)	211 (+37.1)
	EPA	20	344 (+8.7)	317 (-3.6)	277 (+4.6)	235 (-15.1)	211 (+28.1)
		-175	342 (+13.7)	316 (-6.6)	277 (+3.9)	234 (-17.8)	212 (+35.5)
(R)-14	MeOH	22	334 (+6.4)	[285 (-4.2)] ^b	259 (+1.9)	238 (-10.2)	213 (+20.4)
	hexane	22	342 (+6.4)	[300 (-5.1)] ^b	273 (+3.6)	240 (-13.2)	214 (+27.5)
	EPA	20	340 (+7.4)	[292 (-4.0)] ^b	265 (+3.9)	239 (-13.9)	214 (+28.5)
		-175	332 (+8.9)	[288 (-10.8)] ^b	259 (+5.6)	239 (-21.5)	215 (+38.3)

^aTwo overlapping bands. ^bNew band, caused by conjugation with 4-Ph or 5-Ph.

Table XI. Input Data for Calculation of Rotational Strengths

chromophore	transtn and dirctn	energy kK	transtn moments		transtn and static charges ^b MP	QP
			μ/D	M/β^a		
	¹ L _b	38.20	0.225		(2, 6) \pm 0.01530 (3, 5) \pm 0.0044	
	¹ L _a	48.19	2.66		(1) -0.0692 (2, 6) - 0.0309 (3, 5) + 0.0421 (4) + 0.0511	
	¹ B _a	52.91	4.4		(1) - 0.1145 (2, 6) - 0.0511 (3, 5) 0.0697 (4) 0.0846	
	¹ B _b	52.91	4.4		(2, 6) \pm 0.1030 (3, 5) \pm 0.0859 (H _a) - 0.040 ^c (C _{β,γ}) + 0.090 (H _{β,γ}) - 0.030 (C _{δ}) + 0.100 (H _{δ}) - 0.040 (C1) - 0.030 (C2, 6) + 0.033 (H2, 6) - 0.025 (C3, 5) + 0.011 (H3, 5) - 0.018 (C4) + 0.021 (H4) - 0.018	
	n \rightarrow n*	29.33		0.598		(C2) 0.022
	$\pi\rightarrow\pi^*$ $\alpha = 8.8^\circ$ centered in C2 = S6	31.25	4.0		(1) + 0.0477 (2) + 0.0548 (3) + 0.0560 (4) - 0.0416 (5) + 0.0476 (6) - 0.1690	y = z \pm 0.479 Å (S6) 0.184 y = z \pm 1.201 Å
	$\pi\rightarrow\pi^*$ $\alpha = 25^\circ$ centered in C4 = C5	44.50	3.5		(1) - 0.0779 (2) - 0.0033 (3) - 0.0793 (4) + 0.1325 (5) - 0.1107 (6) + 0.1388	

^a β = Bohr magneton = $9.274 \cdot 10^{-21}$ erg/G = $9.274 \cdot 10^{-24}$ J T⁻¹ (Am²). ^bIn units of the electronic charge. ^cStatic charges. ^dLocal coordinates, x axis along C2-S6 bond.

Table XII. Experimental and Theoretical^a Rotational Strengths^b and Free Energy Differences^c

compd conformer	band 1 (n \rightarrow π^*)		band 2 ($\pi\rightarrow\pi^*$)		band 3 (¹ L _b)		band 4 ($\pi\rightarrow\pi^*$)		band 5 (¹ L _a)	
	R_{exp}	R_{theor}	R_{exp}	R_{theor}	R_{exp}	R_{theor}	R_{exp}	R_{theor}	R_{exp}	R_{theor}
1 , major (MII)	-0.26 (0.5) ^c	-0.12	+0.66 (0.5) ^c	+0.11	+0.12	+0.0029	-0.21	-0.38	+0.67	+0.23
minor (MI)	+0.77	+0.17	-0.74	-0.06 ^d						
2 , major (MI)	+0.30 (1.0) ^c	+0.10	-0.05	+0.005 ^d	+0.045	+0.0019	-1.08	-0.087	+1.35	+0.082
minor (MII)	-0.43	-0.18	+0.60	+0.074						
5 , major	-0.07 (0.6) ^c		+0.44 (0.7) ^c		+0.052		-0.35		+0.84	
minor	+0.19		-0.58							
12 , major (MIV)	+0.09 (0.7) ^c	+0.12	+0.02	-0.021 ^d	+0.05	+0.0014	-0.55	-0.19	+1.29	+0.079
minor (MIII)	+0.68	+0.08	-1.13	-0.049						
13 , major (MIII)	+0.16 (1.1) ^c	+0.087	-0.15 (1.1) ^c	-0.041	+0.05	+0.0021	-0.64	-0.17	+1.02	+0.080
minor (MIV)	-0.20	+0.11	+0.23	-0.060 ^d						

^aDielectric constant = 1.0. ^bIn Debye-Bohr magnetons.⁵² ^c $\Delta G^\circ = G^\circ$ (minor) - G° (major) kcal/mol. ^dNear node on rotational strength.

minimum MI (Table VI and Figure 2) is calculated to be lowest in energy, but for **1** MII is predicted to be only 0.57 kcal/mol higher, whereas MII is predicted to be 2.5 kcal/mol higher than MI in **2**. The positions of the minima can be expected to be approximately correctly calculated, but there are grounds to believe that MII is actually lower than MI in the compounds from group 1. One argument is the equality in signs for bands 1 and 2 of the major forms from group 3 with those of the minor forms from group 1. Another is the strong downfield shift of the H-4 reso-

nances in **1**, **5**, and **10** with decreasing temperature (Table VIII). It is obvious (Figure 2) that H-4 is less shielded in MII than in MI because of the different orientations of the benzene ring and the proximity of the rotor methyl in MII (van der Waals shift). Further arguments come from the calculated rotational strengths (vide infra).

Compounds **12** and **13** behave similarly, i.e., the signs of the rotational strengths of bands 1 and 2 in the minor rotamer of **12** correspond to those of the major of **13** and vice versa. The MM

calculations predict two anti minima, MIII and MIV, for each compound, with MIII lowest in energy. For similar reasons as above, it seems as if the energy of MIV in **12** is overestimated and that it is the minimum energy conformation.

The complementarity of the rotational strengths of $n \rightarrow \pi^*$ and $\pi \rightarrow \pi^*$ transitions for many of these compounds, i.e., a negative $n \rightarrow \pi^*$ transition goes with a positive $\pi \rightarrow \pi^*$ transition and vice versa, indicates that the one-electron mechanism²² is important. Its contribution to the total rotational strength is given by $R_{12} = \pm V_{12} [\mu_2 \cdot \mathbf{M}_1] / (\epsilon_1 - \epsilon_2)$, where 1 and the plus sign refer to the magnetically and 2 and the minus sign to the electrically allowed transition. V_{12} is the perturbation energy due to chirally disposed static charges, and ϵ_1 and ϵ_2 are the transition energies. Large contributions from this effect are predicted because of the near parallelity of μ_2 and \mathbf{M}_1 and the similar energies of the two transitions.

The rotational strengths calculated by the Schellman matrix technique (Table XII) show a clear correlation with the experimental values, provided the major rotamer of **1** is assigned to the MII and the major rotamer of **2** to the MI geometry. A picture emerges, in which the compounds from group 1 (**1**, **5**, and **10**) undergo rapid exchange between MI and MII types of minima, MII being more stable by 0.5–0.7 kcal/mol. The compounds in group 3 are involved in similar equilibria, but here MI is more stable than MII by 1.0 kcal/mol or more. The low R values for band 2 and their sign variations are in harmony with the proximity of MI to a nodal line on the rotational strength map for this transition.

The calculations also reproduce the positive sign and low intensity of band 3. Bands 4 and 5 resemble a negative couplet, but calculations with the direction of the transition moment for band 4 taken from CNDO/S or RPA²⁵ calculations ($\alpha = 98.5^\circ$ or 111.9°) give incorrect signs for bands 4 and 5. A series of trial transition moments of the same magnitude but varying direction were then used, and the corresponding transition monopoles were obtained by the Lagrange multiplier technique proposed by Rizzo and Schellman,^{19b} with the scaled CNDO/S monopoles as starting set. With α in the range 5 – 50° , the correct signs were obtained for bands 4 and 5, with the largest amplitude for α ca. 25° . By using this value, a reasonable rendition of bands 4 and 5 is obtained with respect to signs and relative magnitudes of the rotational strengths, whereas the absolute rotational strengths are underestimated (Table XII). The low intensity of the calculated CD bands may be ascribed to deficiencies in the model, e.g., the location of the monopoles. Woody^{26a} points out that Slater orbitals are too contracted and that the monopoles should be more distant from the nuclei. However, at present it does not seem meaningful to try to improve the agreement by variation of these distances.

It should be mentioned that the variation of the direction of the transition moment of band 4 has little effect on the calculated rotational strengths for bands 1, 2, and 3. The numerical discrepancies, especially the low R values for bands 4 and 5 in MI, are possibly related to the existence of one or more magnetically allowed but electrically forbidden transitions in this region, e.g., of $n \rightarrow \sigma^*$ or $\pi \rightarrow \sigma^*$ type. However, at present we are satisfied that the calculations correctly reproduce signs and relative magnitudes of the rotational strengths of bands 1, 2, and 3.

Only in the 4-phenyl compounds **4**, **9**, and **14** do observable populations of the syn rotamer exist, p_{syn} varying from at most 0.17 at $+20^\circ\text{C}$ (for **14**) to 0.01 or less at -170°C . With decreasing temperature, **9** shows only slight increases in intensity with similar bandshape, whereas **4** and **14** show changes in the region 300–380 nm due to weakening of band 1 and strengthening of band 2, both being positive. The absence of isosbestic points in these spectra indicates the existence of more than two conformers.

The tetrahydronaphthalene derivatives **12** and **13** show a similar complementarity of bands 1 and 2 as the compounds of group 1, although with reversed signs, i.e., the bands 1 are positive and the bands 2 negative. Analysis of the temperature dependence of the band areas (Table XII) leads to the assumption of equilibria between mainly two rotamers in each molecule. In **12** the major

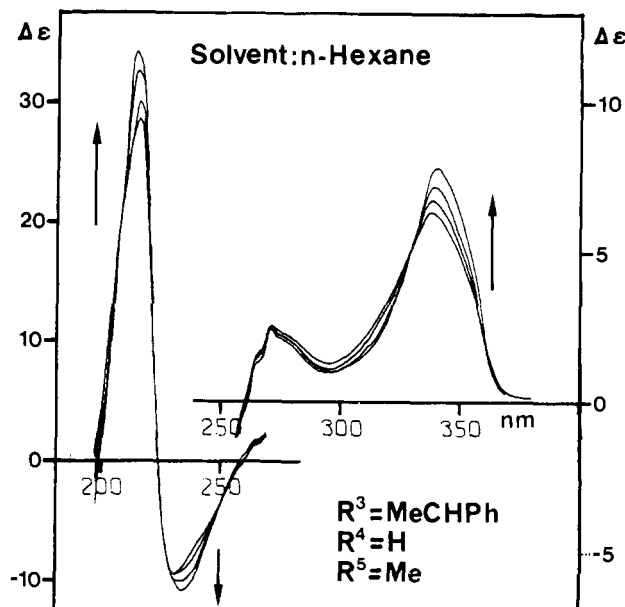


Figure 12. CD spectra of **5** in hexane at $+24$ ($+25$), -5 (-2), -27 , and -51 (-53) $^\circ\text{C}$.

rotamer has low positive R values for both bands and the minor a large positive R for band 1 and a large negative R for band 2, whereas with **13** the situation is essentially reversed. Calculations by the Schellman technique, using the geometries for MIII and MIV, give agreement in sign for all bands when the directions of the benzene 1L_b and 1L_a transition moments are taken from the 1-phenylethyl compounds. If it is assumed that the major rotamer of **12** has the MIV and the minor the MIII geometry and that the reverse is true for **13**, the right orders of magnitudes of the R values for bands 1 and 2 are also reproduced. However, if the directions of the 1L_b and 1L_a transition moments are taken from *o*-xylene (Table XI), the wrong sequence of signs for bands 1–5 ($++--$ instead of $+-+-$) is obtained, and the complementarity of the rotational strengths of bands 1 and 2 is not reproduced. The 1L_b and 1L_a transition moments arise from small differences between rather large transition charges, and they are sensitive to small perturbations of the charges. It is reasonable to assume that the carbon atom, which carries the thiazolinethione ring, affects the transition charge distribution more than the other bridge carbon atom, i.e., that toluene is a better model than *o*-xylene for the transitions in the benzene ring in **12** and **13**.

The assignment of geometries MIII and MIV to the rotamers of **12** and **13** is also in agreement with the NMR data (Table VIII). The downfield shift of the H4 resonance of **12** with decreasing temperature is explained by the orientations of the benzene ring, MIII being the geometry with least deshielding of H4. The lower J_+ value for **12** is also in agreement with the dominance of MIV with a pseudoaxial substituent.

Notable effects on bands 1 and 2 are observed for the compounds of group 1 (**1**, **5**, and **10**) when going from methanol, dichloromethane, or EPA to hexane as solvent. For **1** and **5** (Figure 12), broad positive bands appear with λ_{max} 337 and 338 nm, respectively, non-Gaussian but apparently with only little contribution from the bands at 320 and 322 nm, respectively. For **10** a strong positive band is seen at 366 nm with a shoulder on the short-wavelength side and with a weak negative band at 330 nm. These results are consistent with predominance of a rotamer of type MI in hexane solution.

Conclusion

Summing up the results of the analysis of the temperature-dependent NMR and CD spectra, and X-ray crystallographic results, and the molecular mechanics calculations we find that compounds **1**–**14** exist predominantly in the anti form.

Two types of rotamers with free energy differences of 0.7–1.0 kcal/mol, separated by low barriers and both within the anti form,

seem to exist in most compounds, one type being the major rotamer in the 4-H compounds **1**, **5**, **10**, and **12** but the minor rotamer in the four-substituted analogues. This type of double minima within one main conformer has often been inferred from molecular mechanics calculations,⁴⁰ but this is the first experimental proof for their existence. The MM2 force field is unexpectedly unsuccessful in predicting conformational energies, but the calculated minimum energy geometries are believed to be more reliable.

Acknowledgment. We thank the Swedish Natural Science Research Council, the French Centre National de la Recherche Scientifique, and the Knut and Alice Wallenberg Foundation for generous financial support. We also thank Dr. T. Liljefors for helpful advice with the molecular mechanics calculations, J. Glans for skillful recording of the CD spectra, Dr. I. Nilsson and Professors J. A. Schellman and G. Pfister-Guillouzo for making their computer programs available to us and for much good advice, and

Professor T. D. Bouman and Dr. A. E. Hansen for providing us with data prior to publication.

Registry No. **1**, 96393-05-4; **2**, 96393-06-5; **3**, 105615-74-5; **4**, 105615-75-6; **5**, 105519-59-3; **6**, 105615-76-7; **7**, 105615-77-8; **8**, 105615-78-9; **9**, 105519-60-6; **10**, 105615-79-0; **11**, 105519-61-7; **(±)-12**, 96349-15-4; **(±)-13**, 96349-16-5; **(±)-14**, 96349-17-6; **15**, 17294-24-5; *(R)*-*N*-(1-phenylethyl)ammonium *(R)*-*N*-(1-phenylethyl)dithiocarbamate, 105660-54-6; *(R,S)*-1-amino-1,2,3,4-tetrahydronaphthalene, 32908-38-6; triethylammonium *(R,S)*-*N*-(1,2,3,4-tetrahydro-1-naphthyl)dithiocarbamate, 105519-63-9; chloroethanal, 107-20-0; 1-phenyl-2-bromoethanone, 70-11-1; 2-bromo-4-methyl-3-pentanone, 29583-93-5; 2-bromo-2-phenylethanal, 16927-13-2; 1-phenyl-2-bromo-1-propanone, 2114-00-3; *(S)*-*N*-(1-phenylethyl)ammonium *(S)*-*N*-(1-phenylethyl)dithiocarbamate, 105519-65-1; CS₂, 75-15-0; *(R)*-1-phenylethylamine, 3886-69-9; chloropropanone, 78-95-5; 3-chloro-2-butanone, 4091-39-8; 1-bromo-3-methyl-2-butanone, 19967-55-6; 2-bromo-3-pentanone, 815-52-1; 1-bromo-1-phenyl-2-propanone, 23022-83-5; 2-bromopropanal, 19967-57-8.

Photooxidation of Tetraanionic Sensitizer Ions by Dihexadecyl Phosphate Vesicle-Bound Viologens

James K. Hurst,*† David H. P. Thompson,† and John S. Connolly†

Contribution from the Department of Chemical and Biological Sciences, Oregon Graduate Center, Beaverton, Oregon 97006-1999, and Photoconversion Research Branch, Solar Energy Research Institute, Golden, Colorado 80401. Received July 2, 1986

Abstract: Triplet state lifetimes of several photoredox-active anions were shortened by adding *N*-alkyl-*N*'-methyl-4,4'-bipyridinium (C_nMV²⁺) ions in the presence of dihexadecyl phosphate (DHP) vesicles. Optical spectroscopic measurements indicate that the predominant reaction mechanism is one-electron oxidative quenching. For [5,10,15,20-tetrakis(4-sulfonatophenyl)porphinato]zinc(II) (ZnTPPS⁴⁻) ion, yields of charge-separated product ions are high, so that overall quantum yields exceeding 0.5 redox pairs per photon absorbed can be realized; for tetrakis(diphosphito)diplatinate(II), tris(4,7-bis(4-sulfonatobenzyl)-1,10-phenanthroline)ruthenate(II), and tris(4,4'-dicarboxylato-2,2'-bipyridine)ruthenate(II) yields are markedly less, a consequence of their shorter intrinsic triplet lifetimes and poor cage escape yields. In the absence of vesicles, product formation is negligible because ion pairing of viologens with sensitizers is extensive, giving rise to static quenching of the photoexcited states. The ionic strength dependence of the kinetics of ³ZnTPPS⁴⁻ ion oxidation by C_nMV²⁺-DHP particles suggests a diffusion-controlled mechanism with electron transfer occurring over a distance of separation approximating the hard-sphere collision diameter of sensitizer and viologen. Although the quenching rate constants are determined by the frequencies of collision between vesicles and ³ZnTPPS⁴⁻, an apparent concentration dependence upon C_nMV²⁺ ions arises because the effective dielectric constant at the reaction site varies with the extent of viologen loading. Recombination of the ZnTPPS³⁻ π-cation with viologen radical cations follows mixed first- and second-order kinetics; possible mechanisms are discussed.

Interfacial adsorption and partitioning reactants between solution microphases are techniques that have been used to modify the chemical reactivity of a wide variety of processes, including photochemical redox reactions.¹ The physical state(s) of the adsorbed reactants are often not well-characterized, particularly when both microphases are fluid, rendering quantitative interpretations of their dynamic behavior difficult. For example, the extent of aggregation of minor components in synthetic mixed vesicles has been shown in several systems to depend upon medium composition, dopant levels, and the structural phase of the vesicles.² Furthermore, the simultaneous presence of two or more distinct binding sites within a single vesicle has been inferred from the chemical³⁻⁵ and photophysical⁶⁻⁹ behavior of a variety of adsorbed substances. Thus, despite the apparent simplicity of these microphase assemblies, their physical properties and dynamic behavior suggest considerable structural heterogeneity of bound reactants.

As part of our effort to develop a conceptual understanding¹⁰ of the phenomenon of transmembrane oxidation-reduction across bilayer membranes^{3,11-15} we have sought to characterize the nature

of binding of alkylviologens (*N*-alkyl-*N*'-methyl-4,4'-bipyridinium, C_nMV²⁺) to anionic dihexadecylphosphate (DHP) vesicles. In

(1) Representative reviews: Fendler, J. H. *Annu. Rev. Phys. Chem.* **1984**, *35*, 137-151. Grätzel, M. *Mod. Aspects Electrochem.* **1983**, *15*, 83-165. Thomas, J. K. *ACS Symp. Ser.* **1982**, *198*, 335-346. Kuhn, H. *Pure Appl. Chem.* **1979**, *51*, 341-352.

(2) Kunitake, T.; Ihara, H.; Okahata, Y. *J. Am. Chem. Soc.* **1983**, *105*, 6070-6078. Nakashima, N.; Morimitsu, K.; Kunitake, T. *Bull. Chem. Soc. Jpn.* **1984**, *57*, 3253-3257.

(3) Ford, W. E.; Tollin, G. *Photochem. Photobiol.* **1983**, *38*, 441-449.

(4) Mizutani, T.; Whitten, D. G. *J. Am. Chem. Soc.* **1985**, *107*, 3621-3625.

(5) Ishiware, T.; Fendler, J. J. *J. Am. Chem. Soc.* **1984**, *106*, 1908-1912.

(6) Suddaby, B. R.; Brown, P. E.; Russell, J. C.; Whitten, D. G. *J. Am. Chem. Soc.* **1985**, *107*, 5609-5617.

(7) Schanze, K. S.; Shin, D. M.; Whitten, D. G. *J. Am. Chem. Soc.* **1985**, *107*, 507-509.

(8) Almgren, M. *J. Phys. Chem.* **1981**, *85*, 3599-3603.

(9) Cellarius, R. A.; Mauzerall, D. *Biochim. Biophys. Acta* **1966**, *112*, 235-255.

(10) Hurst, J. K.; Thompson, D. H. P. *J. Membrane Sci.* **1986**, *28*, 3-29.

(11) Mettee, H. D.; Ford, W. E.; Sakai, T.; Calvin, M. *Photochem. Photobiol.* **1984**, *39*, 679-683, and earlier publications cited therein.

(12) Lee, L. Y. C.; Hurst, J. K. *J. Am. Chem. Soc.* **1984**, *106*, 7411-7418.

(13) Runquist, J. A.; Loach, P. A. *Biochim. Biophys. Acta* **1981**, *637*, 231-244.

*Oregon Graduate Center.

†Solar Energy Research Institute.